NASA CR 120884

STUDY OF MECHANISM WHICH CAUSES FILM FORMATION ON MERCURY SURFACES

by

Geoffrey Frohnsdorff and Diane Dunn

THE GILLETTE COMPANY RESEARCH INSTITUTE

prepared for

National Aeronautics and Space Administration

CONTRACT NAS3-14363

NASA Lewis Research Center
Cleveland, Ohio 44135
Eugene P. Symons, Project Manager
Chemical Propulsion Division

1. Report No.	2. Government Accession No.	3. Recipient's Catalog No.
NASA CR-120884		

4. Title and Subtitle	5. Report Date
STUDY OF MECHANISM WHICH CAUSES FILM FORMATION ON MERCURY SURFACES	March 1972
	6. Performing Organization Code

7. Author(s)	8. Performing Organization Report No.
Geoffrey Frohnsdorff and Diane Dunn	10. Work Unit No.

9. Performing Organization Name and Address	11. Contract or Grant No.
The Gillette Company Research Institute 1413 Research Boulevard Rockville, Maryland 20850	NAS 3-14363

12. Sponsoring Agency Name and Address	13. Type of Report and Period Covered
National Aeronautics and Space Administration Washington, D. C. 20546	Contractor Report
	14. Sponsoring Agency Code

15. Supplementary Notes

Project Manager, E. P. Symons, Chemical Propulsion Division
NASA Lewis Research Center, Cleveland, Ohio

16. Abstract

The purpose of the program was to determine the mechanism by which small quantities of dissolved tin, sodium and lithium lower the rate of evaporation of mercury in vacuum. An apparatus was built in which dilute amalgams could be prepared and studied in an oxygen-free environment before being exposed to oxygen under controlled conditions. The apparatus was able to maintain a pressure of less than 1.3×10^{-6} N/m^2 (10^{-8} torr) of gases and vapors other than mercury and less than 1.3×10^{-8} N/m^2 (10^{-10} torr) partial pressure of oxygen; also, it provided for mechanical sweeping of the liquid metal surfaces in the vacuum environment. The rates of evaporation of pure mercury and of dilute amalgams of tin (52 ppm), sodium (229 ppm) and lithium (165 ppm) were determined at temperatures between 25° and 55°C both before and after 70 minute exposures to an approximately 270 N/m^2 (2 torr) pressure of oxygen. The rates of evaporation of the pure mercury and the amalgams as first prepared were similar but the rates for the amalgams were reduced by at least 80% at 25°C as a result of the exposure to oxygen. The effect of the oxygen treatment could be completely removed by sweeping the amalgam surfaces. It was concluded that the reduced rates of evaporation resulted from the formation of transparent, insoluble, oxide films on the amalgam surfaces.

17. Key Words (Suggested by Author(s))	18. Distribution Statement
mercury amalgams evaporation oxygen	Unclassified - Unlimited

19. Security Classif. (of this report)	20. Security Classif. (of this page)	21. No. of Pages	22. Price*
Unclassified	Unclassified	74	$3.00

* For sale by the National Technical Information Service, Springfield, Virginia 22151

TABLE OF CONTENTS

Page

SUMMARY

INTRODUCTION. 1

LIST OF SYMBOLS 2

BACKGROUND INFORMATION. 4

CONSTRUCTION, CHECK-OUT AND METHOD OF USE OF THE EQUIPMENT FOR THE EVAPORATION MEASUREMENTS. 7

- The Design and Components of the Equipment 7
- Initial Check-out of the Equipment 9
- Characteristics and Uses of the Pressure Gauges. 9
- Measurement of Vapor Pressures and Evaporation Rates 10
- Temperature Control and Measurement. 12

MEASUREMENTS ON PURE MERCURY. 14

MEASUREMENTS ON AMALGAMS. 17

1. Tin Amalgam 18
2. Sodium Amalgam. 20
3. Lithium Amalgam 23
4. Final Measurements on Mercury 26

GENERAL DISCUSSION. 27

- Relative Evaporation Rates 27
- Absolute Evaporation Rates in the Evaporation Chamber and in Free Space 29

CONCLUDING REMARKS. 32

SUMMARY OF RESULTS. 33

REFERENCES. 35

TABLES 1 - 11

FIGURES 1 - 17

TABLE OF CONTENTS (Concluded)

Page

APPENDIX I - Surface Excess Concentrations of Alkali Metals in Amalgams

APPENDIX II - Materials

APPENDIX III - Calculation of the Meniscus Surface Area and Volume from the Meniscus Weight

APPENDIX IV - Temperature Corrections

APPENDIX V - Analysis of Amalgams

APPENDIX VI - The Effective Pressure above the Meniscus in the Evaporation Experiments

DISTRIBUTION LIST

SUMMARY

This report describes a program aimed at establishing the mechanism by which small quantities of dissolved impurities, specifically tin, sodium and lithium, lower the rates of evaporation of mercury in vacuum. At the start of the program, an ultra-high vacuum system with the special features needed for evaporation rate measurements was built. It was designed so that pure mercury and dilute amalgams could be prepared and studied in an oxygen-free environment ($< 1.3 \times 10^{-8}$ N/m^2 partial pressure of O_2) before being exposed to oxygen under controlled conditions. A feature of the equipment was that the liquid surface in the vacuum system could be cleaned by mechanical sweeping. The apparatus was used for evaporation rate measurements on pure mercury and three amalgams. The amalgams contained, respectively, 52 ppm tin, 229 ppm sodium, and 165 ppm lithium.

For each of pure mercury and the amalgams, evaporation rate measurements were made at 25°, 40° and 55°C on the liquids (i) as first prepared, (ii) after sweeping of the surface, (iii) after exposure to oxygen, and (iv) after sweeping the surface again.

The results showed that the rates of evaporation of pure mercury and of the three amalgams were the same within the approximately 15% limits of experimental error over the 25° to 55° temperature range. They also showed that exposure to an approximately 270 N/m^2 pressure of oxygen for 70 minutes reduced the rates of evaporation of the amalgams at 25°C by at least 80% but it had no effect upon the pure mercury. The lowered rates of evaporation, at least for the sodium and lithium amalgams, were due to the formation of thin, transparent, insoluble, films which only became visible when they buckled as the surface area of the liquid was reduced. Further, the films on the amalgam surfaces could be removed and the evaporation rates restored to their original values by sweeping the surfaces.

While most of the results were comparative, one set of absolute measurements of the rates of evaporation of the sodium amalgam was made volumetrically. By combining the results of these absolute measurements with the relative ones, it was possible to deduce the rates of evaporation of each of the amalgams and pure mercury in free space. The values for pure mercury were (in g.cm^{-2}.sec^{-1}), 1.0×10^{-4} at 25°C, 3.0×10^{-4} at 40°C, and 8.5×10^{-4} at 55°C.

The rates of evaporation of the oxygen-free amalgams were the same as for the mercury within the experimental error and it was concluded that the vapor pressures of the amalgams and the mercury were also the same within the experimental error.

INTRODUCTION

Mercury is a candidate liquid metal for use in some components of space vehicles. In particular, it is being considered for use in sliding contacts connecting the solar cells to the other electrical components of the direct broadcast television satellite being studied by NASA. A major limitation on the usefulness of pure mercury for this application is its undesirably high rate of evaporation under the hard vacuum conditions of outer space.

In studies carried out for NASA at The Gillette Company Research Institute between 1968 and 1970 (1,2), it was shown that low concentrations of soluble metallic impurities in mercury can cause films to form on the mercury surface which will lower the rate of evaporation in vacuo by more than 99%. Among the metals which produced at least a 99% reduction in the evaporation rate of mercury, when present at about 200 ppm by weight, were tin, lithium and sodium. However, the earlier work did not establish the mechanism responsible for the lowered rates of evaporation and it was therefore not certain whether the mecahnism would be operative in outer space even though it was in a laboratory apparatus capable of achieving a vacuum of 10^{-3} to 10^{-4} N/m^2. The possible mechanisms were considered to be: (i) formation of a Gibbsian adsorbed layer of a soluble species, whether metal, intermetallic compound, or oxide; and (ii) formation of a surface layer of an insoluble compound, e.g. an insoluble oxide. (The possibility of occurrence of oxides could not be ruled out because of the difficulty of obtaining the metals in perfectly clean form and because of the probable occurrence in the vacuum system of at least enough oxygen to form a monolayer of oxide on the amalgam surfaces.)

The first of the two types of mechanism would have the advantage that the surface layer would be inherently self-healing if disturbed. The second would probably only be self-healing if oxygen, or some other oxidizing agent, were present to cause the formation of more insoluble material to replace any which was displaced from the surface. Either mechanism could be useful in spacecraft applications, but it is necessary to know the mechanism if the optimum design is to be achieved. It is, of course, possible that different metals lower the rate of evaporation of mercury by different mechanisms.

The purpose of the work described in the present report was to determine the mechanism which causes the formation of a film on the surface of liquid mercury to which trace amounts of tin, lithium and sodium have been added. A more specific objective was to determine if the mechanism which causes the film formation would permit the regeneration of a new film should the original film be disrupted in the absence of oxygen.

The report is divided into five main sections. The first, the introduction, includes a list of symbols and background information pertinent to the later parts. This is followed by a description of the apparatus used and by two sections devoted to the measurements, one on pure mercury and one on the amalgams. Finally, there is a general discussion in which all of the results are reviewed and interpreted.

LIST OF SYMBOLS

A	area of meniscus or orifice (cm^2)
C_2	concentration of solute (moles/l.)
F	conductance of tube ($cm^3.sec^{-1}$)
G	rate of evaporation per unit area ($g.cm^{-2}.sec^{-1}$)
G_{cap}	rate of capture of molecules per unit area ($g.cm^{-2}.sec^{-1}$)
G_{ec}	rate of evaporation per unit area (as measured in the evaporation chamber) ($g.cm^{-2}.sec^{-1}$)
G_{esc}	rate of escape of molecules per unit area ($g.cm^{-2}.sec^{-1}$)
G_{fs}	rate of evaporation per unit area in free space ($g.cm^{-2}.sec^{-1}$)
K	constant in equation for calculation of F
M	gram molecular weight ($g.mole^{-1}$)
P	pressure (newton/m^2 or torr; 1 torr = 133.5 N/m^2)
P_c	pressure at level at which condensation occurs (N/m^2)
P_{ig}	pressure indicated by the ionization gauge (torr)
P_{sat}	saturation vapor pressure (N/m^2)
Q	rate of flow of mercury vapor ($g.sec^{-1}$)
R	the gas constant ($joule.deg^{-1}.mole^{-1}$)
R_e	rate of evaporation from the total area of the meniscus ($g.sec^{-1}$)
T	temperature (°C or °K)
T_c	wall temperature at level at which condensation occurs (°C)
T_m	meniscus temperature (°C)
T_w	wall temperature (°C)
V	meniscus volume (cm^3)
V_a	average velocity of gas molecule ($cm.sec^{-1}$)
d	diameter of evaporation chamber (cm)

h	meniscus height (cm)
v	volume evaporated (cm^3 or μl)
t	time (duration of experiment) (sec)
x	distance between meniscus and level at which condensation occurs (cm)
Γ_2	surface excess concentration ($moles.cm^{-2}$)
ΔT	temperature difference (°C)
γ	surface tension ($dynes.cm^{-1}$)

BACKGROUND INFORMATION

The net rate of evaporation of a liquid is the difference between the rates at which molecules leave and enter the surface, to and from the vapor phase. The rate at which molecules leave the surface is governed by the area of the liquid-vapor surface, the heat of vaporization and the kinetic energy distribution of the molecules in the liquid. The heat of vaporization is governed by the intermolecular forces between the molecules in the liquid and the kinetic energy is governed by the temperature. It is generally believed that evaporation of a molecule from a condensed phase proceeds by two more or less distinct steps: (i) migration from the bulk into the surface and (ii) escape from the surface. If this is so, then the composition of the surface layer should be an important factor in governing the rate of escape.

The rate at which molecules of a pure liquid enter the surface from the pure vapor phase is generally the same as, or very close to, the rate at which they hit the surface. This must be true for pure mercury in the temperature range of interest here since its accomodation coefficient has been shown to be unity from -30° to 60°C (3). The rate of capture, G_{cap}, by the surface can be calculated from the kinetic theory of gases and may be shown to be (4):

$$G_{cap} = 4.410 \cdot 10^{-4} \cdot P \cdot \left(\frac{M}{T}\right)^{\frac{1}{2}} g.cm^{-2}.sec^{-1} \qquad (1)$$

where P is the pressure in N/m^2, M the molecular mass in grams, and T the absolute temperature in degrees Kelvin. This is an important relationship since, at the saturation pressure, the rates of escape from and capture by the surface must be equal. Thus, the rate of escape, G_{esc}, which is generally believed not to change significantly with the pressure of the vapor (4), can be written:

$$G_{esc} = 4.410 \cdot 10^{-4} \cdot P_{sat} \cdot \left(\frac{M}{T}\right)^{\frac{1}{2}} g.cm^{-2}.sec^{-1} \qquad (2)$$

where P_{sat} is the saturation vapor pressure (in N/m^2) at T°K, and the net rate of evaporation can be expressed:

$$G = G_{esc} - G_{cap} = 4.410 \cdot 10^{-4} \cdot \left(P_{sat} - P\right) \cdot \left(\frac{M}{T}\right)^{\frac{1}{2}} g.cm^{-2}.sec^{-1} \qquad (3)$$

The quantity G_{esc} in equation (2) defines the rate of evaporation which can be achieved from the surface of a pure liquid in free space, while G in equation (3) expresses the net rates of evaporation at finite pressures of the vapor. G_{esc} is the quantity which is of greatest interest from the point of view of the present investigation though it is G that is measured directly.

Applying equation (2) to the evaporation of mercury at 25°C (298°K), knowing its saturation vapor pressure at this temperature to be 2.76×10^{-1} N/m^2 (5) it may be calculated that the rate of evaporation in free space should be 1.0×10^{-4} $g.cm^{-2}.sec^{-1}$.

Whereas equations (2) and (3) can be applied to the cases of pure liquids and solids, they cannot always be applied to surfaces covered by films of surface active materials. Thus, it is well known that the rate of evaporation of water can be significantly reduced by monolayers of some high high molecular weight fatty acids and alcohols (6), even though the vapor pressure of the water is not changed. The explanation is that the film lowers the rates of escape and capture equally by the introduction of a barrier of low permeability between the liquid and vapor.

While some surface films act as barriers to evaporation, not all do so. Examples of monolayers which do not measurably retard the evaporation of water from aqueous media are protein layers on water (7) and layers of n-octadecylamine on 0.01N sulfuric acid solution (8). The effectiveness of layers in retarding evaporation of water depends upon the closeness of packing of the molecules in the surface layer and upon the length of the hydrocarbon chains in the molecules. The effectiveness is high for long chain normal saturated fatty acids but it is lowered by the replacement of hydrogen atoms in the alkyl group by halogen atoms or other groups such as hydroxyl which hinder the closest packing. Small quantities of impurities in the retarding material can also reduce its effect.

The effect of solutes upon evaporation of the solvent is usually considered to be due to their effects on the solvent vapor pressure. For solutions which approximate to ideality, the vapor pressure lowering can be calculated from Raoult's law (9), i.e. the lowering is directly proportional to the reduction in mole fraction of the solvent. However, many amalgams, particularly those of the alkali metals, show large negative deviations from Raoult's law with the mercury vapor pressures over concentrated amalgams being far below the predicted values. Thus, Poindexter (10) calculated the vapor pressure of mercury over a 50% mole fraction sodium amalgam at 20°C to be 4×10^{-6} N/m^2 whereas, if the solution were ideal, the pressure should have been about 9×10^{-2} N/m^2. For dilute amalgams (e.g. <1% of solute), the vapor pressures of mercury above them do not differ much from the values predicted by Raoult's law (11,12). Thus, any large reduction in the rate of evaporation of a dilute amalgam cannot be attributed to the reduced vapor pressure.

The alkali metals are strongly surface active in solution in mercury but tin is less so. A comprehensive review of the effects of dissolved metals on the surface tension of mercury has been given by Semenchenko (13). It has not been established whether the high surface excess concentrations of the alkali metals have a marked effect on the rate of evaporation. Surface excess concentrations calculated from the Gibbs equation show that the accumulation of alkali metals in the surface regions even of dilute amalgams could be sufficient to produce a quite high concentration of alkali metal atoms if they were localized in the surface (see Appendix I). Independent evidence for the occurrence of high concentrations of alkali metal atoms (or ions) in dilute amalgams was obtained by Pohl and Pringsheim (14) who showed that the surface of a 2×10^{-4} atom % (0.4 ppm by weight) potassium amalgam had the photo-emission characteristics of pure potassium. If the

surface layer of a dilute amalgam contains a high proportion of adsorbed atoms or ions, it seems possible that this could reduce the rate of evaporation of mercury to below that predicted from the vapor pressure and equations (2) and (3).

Whereas surface composition in terms of soluble surface active species might possibly affect evaporation rates of amalgams, it is also possible that insoluble layers such as oxides on the surface might do so. The oxidation of metals has been studied intensively over many years, particularly in connection with corrosion. Most metals spontaneously form oxide or other coatings on exposure to air at ambient temperature, the coatings often being very thin but sufficiently dense to almost completely inhibit further reaction (15). Such coatings appear to be barriers to the migration of oxygen or other reactive species to the metal surface. Pure mercury is one of the relatively few metals which does not appear to form an oxide coating when exposed to air at ambient temperature (3,15). However, it is well known that mercury containing dissolved metallic impurities often shows signs of reaction with the atmosphere by the formation of a scum (1,16). In a study relevant to the present report, Feldmann (17) showed that sodium amalgam reacted with oxygen at ambient temperature and 10 atmospheres pressure to give a quantitative yield of sodium peroxide. Presumably such an oxide, if formed as a dense coating over an amalgam surface, could reduce the rate of evaporation.

In studies of surface films on liquids, it is important to be able to achieve clean surfaces on the liquids to provide points of reference against which to assess the effects of the films. A well-established technique for the removal of insoluble surface layers without removing the liquid itself is to sweep the surface with a barrier which penetrates the surface over its whole width (6). Another technique which has been shown to be effective in preparing clean surfaces of mercury for gas adsorption studies is to cause the overflow of the mercury from its container so as to carry surface contamination with the overflow (18). Both of these techniques have influenced the method of cleaning used in the present work.

The quantitative intercomparison of low pressures of vapor was a requirement for the program described in this report. A method which is frequently used in the continuous monitoring of a system without significantly perturbing its state is to leak vapor from it through a small orifice to a sensitive quantitative gas detector such as an ionization gauge or mass spectrometer. If the pressures on both sides of the orifice are in the molecular flow range, and if the geometry and pumping characteristics of the downstream portion of the system are held constant, the pressure at the gauge is proportional to the pressure on the up-stream side of the orifice (19). Such systems have been used for determination of the heat of vaporization of materials of low volatility by determination of the temperature variation of vapor pressure and application of the Clausius-Clapeyron equation to the data. In the present work, determination of the heat of vaporation of mercury was used as a check on the internal consistency of the measurements and the method of treatment of the data. Values for the heats of vaporization and other characteristic properties of mercury, tin, sodium and lithium are given in Table 1.

CONSTRUCTION, CHECK-OUT AND METHOD OF USE OF THE EQUIPMENT FOR THE EVAPORATION MEASUREMENTS

The Design and Components of the Equipment

The purposes of the equipment were to:

(i) prepare oxygen-free pure mercury and amalgams of known concentration;

(ii) determine the relative vapor pressures of pure mercury and of the amalgams at 25°C;

(iii) determine the rates of evaporation from as-prepared and cleaned surfaces of the amalgams and pure mercury at 25, 40 and 55°C, both before and after exposure to a finite pressure of oxygen. The exact sequence of operations to be carried out was mentioned in the Introduction and will be described in more detail in the later sections of this report.

Specific performance requirements of the equipment were that is should be capable of maintaining within it a pressure less than 1.3×10^{-6} N/m^2 (10^{-8} torr) of gases and vapors other than mercury. The pumping and pressure measuring system was purchased as a complete unit built up from standard stainless steel ultra-high vacuum components but with modifications, where necessary, to ensure satisfactory performance in the presence of the expected pressures of mercury vapor. The remainder of the system was constructed almost entirely of borosilicate glass. A photograph of the system prior to the first measurements is shown in Figure 1.

The pumping and pressure measuring system is shown schematically in Figure 2. It consisted of a 3.8 cm i.d. manifold built up from standard flanged stainless steel fittings using corner-sealed copper gaskets. Connected into the manifold for pressure measurements and system monitoring were a Bayard-Alpert type ionization gauge tube with a thoria-coated iridium filament, and also a low resolution mass spectrometer (residual gas analyzer). Of six stainless steel, bellows-sealed valves providing access to the manifold, valves 1, 2 and 4 were connected, through stainless steel bellows, to the glass portion of the system, while valve 3 could be used to isolate the pressure gauges while pumping through valve 6 or opening the system to the air or to an oxygen supply through valve 5. The flanges on the manifold side of valves 1 and 2 carried special nickel-plated copper disks which served as gaskets but also, through small holes bored at their centers, as leaks to the gauges.

The pumps were a 50 l/s ion pump and a sorption pump. All of the pumping and pressure measuring system, apart from the sorption pump and the valves to it, was mounted in a specially constructed, electrically-heated, furnace with demountable sides so that it could be baked at temperatures up to 250°C. The furnace was constructed from a 3.8 cm angle iron frame with sides, top and bottom of 1.3 cm or 2.5 cm thick asbestos-cement board insulated with 2.5 cm of glass wool covered with another, thinner layer of

asbestos-cement board. Seven 76 cm long, 1 KW, strip heaters were mounted with three equally spaced in parallel array 2.5 cm above the furnace bottom and with one along each side at a height of 7.5 cm from the bottom. Control of the heaters was provided by a temperature indicating controller and, as a fail-safe protection against overheating, an override control was provided by a bimetallic strip controller.

The glass portion of the system was mounted on a grid attached to the top of the furnace for the pumping and pressure measuring system. It was modified from time to time as the needs of the work dictated. Its original configuration for the first measurements on pure mercury was as in Figure 3, except that the flange joint carrying the boat for evaporation of the metal for amalgamation was replaced by a glass cap since the first experiment was to be with pure mercury. Like the metal portion of the system, the glassware could be baked out at temperatures of at least 250°C by enclosing it in a specially built demountable furnace of similar construction to that for the metal part.

The features of the glass apparatus can be conveniently described by reviewing how it was used. After leak testing and baking out, the portion of the system above and to the left of break seal BS1 was under vacuum ready for the start of an experiment. Then pure mercury was poured into flask F1, capacity 250 cc, through the side arm which was then connected, through a liquid nitrogen trap, to an auxiliary high vacuum system. The mercury in F1 was then refluxed under vacuum for about one hour in order to degas it and the walls of the flask. The thick-walled glass tubing at S1 was then sealed off with a flame and the mercury was allowed to cool. Next, seal BS1 was opened by use of the magnetic hammer MH1 and the bulk of the mercury was distilled from flask F1 into the similar flask F2. Seal S2 was then closed off with a flame to leave the redistilled mercury in F2 and to isolate the system from F1 which was no longer needed. At this point, in two of the amalgam experiments, the metal in the tantalum boat in the 1 liter flask F3 was evaporated by electrical heating using heavy copper leads through the flange joint, J. When it was judged that enough metal had been deposited on the walls of F3, the evaporation was stopped and mercury from F2 was distilled into F3 to dissolve some of the evaporated metal and to overflow into the reservoir R formed by the lower end of the sloping tube T1. The dissolution of the metal in F3 could be assisted by stirring with the magnetic stirrer bar MS1, or by using the bar to remove metal from the otherwise untouched steeper regions of the walls by scraping or by raising drops of mercury to its level to amalgamate with it. Periodically, the distillation of mercury through F3 and into R was stopped and a sample of the amalgam in R was removed for analysis. The sample was taken by using the magnetic scoop MS2 first to stir the amalgam in R, then to transfer about 1 cc to the lowest of the capsules A. The capsule was sealed off with a flame so that the sample could be removed without breaking the vacuum. On the basis of the analytical results, it was then decided whether to wash more of the trace metal from F3, to dilute the amalgam in R by direct distillation of mercury into R after closing off seal S3, or to use the amalgam without further change.

When the amalgam in R was judged ready for use in the evaporation experiments, scoop MS2 was used to transfer the amalgam to the tube T2 until the level just reached the ground horizontal surface of the precision bore capillary C. The height of the meniscus in C was then adjusted so as to project above C for 1 to 2 mm by movement of the magnetic plunger MS3. The magnetically-operated ball joint valve B1 was closed and the vapor pressure or the rate of evaporation of the amalgam from the meniscus was then determined. For the evaporation measurements, the lower end of the wide bore evaporation tube T3 was surrounded by liquid nitrogen to trap the mercury which evaporated from the meniscus. The trap served the dual purpose of maintaining a high rate of pumping for the mercury vapor and allowing the evaporation tube to be pumped out continuously during the experiments while protecting the ion pump and the gauges from mercury vapor.

Initial Check-out of the Equipment

When the equipment had been assembled, it was tested for its ability to meet the requirements of the project. It was baked out for 24 hours at 250°C. After the system had cooled, the ultimate vacuum recorded by the ion pump was 2.7×10^{-7} N/m^2 and that recorded by the ionization gauge was 2.1×10^{-6} N/m^2. The residual gas analyzer gave the following indications of the partial pressure (N/m^2) of the gases remaining in the system: N_2, 0.9×10^{-7}; A, 0.3×10^{-7}; Ne, 0.5×10^{-7}; He, 1.3×10^{-7}; H_2O, 1.5×10^{-7}; $CO_2 < 10^{-8}$; H_2, 1.2×10^{-7}; O_2, not detectable ($< 10^{-8}$). These pressures were calculated from the gauge readings and the calibration factors provided by the manufacturers. When summed, they indicated a total pressure of 5.7×10^{-7} N/m^2. This was only about one-third of the ionization gauge reading. (Subsequent calculations made to correct the ionization gauge reading for a gas mixture in the ratios indicated by the mass spectrometer suggested that the total pressure was 3.8×10^{-6} N/m^2.)

The leak rate on the glass portion of the system was determined by measuring the pressure build-up in it when closed off from the pump for several hours. The leak rate was calculated to be 7×10^{-15} moles·sec^{-1}. The gas detected by the mass spectrometer was predominantly nitrogen. Assuming that the pressure build-up represented a real leak of air and that the amount of oxygen which had entered the system was 25% of the quantity of nitrogen, it was calculated that it would take 8 days for enough oxygen to enter the system to form a single close packed layer of oxygen molecules on 1 sq cm area of surface. From these considerations, it was concluded that the system was satisfactory for the measurements on pure mercury.

Characteristics and Uses of the Pressure Gauges

According to the manufacturer, the ionization gauge had a sensitivity of 750μA per N/m^2 for nitrogen and had a working range from 1.3×10^{-8} to 2.7×10^{-1} N/m^2. The manufacturer's accumulated experience on ionization gauge performance suggests that the sensitivity seldom changes by more than 20% over the life of a gauge (20). In order to obtain reproducible results, the gauge filament was always turned on for at least an hour before critical

measurements were to be taken and the gauge was degassed for ten minutes prior to the measurements. The gauge zero and the filament current were checked periodically. Evidence to be mentioned in the Discussion section suggests that the gauge sensitivity fell by about 40% during the course of the study.

The mass spectrometer was a 1 cm radius, 180° magnetic deflection instrument. Two main ranges of mass numbers could be scanned with it. These were 12 to 60 and 48 to 240. The manufacturers stated the minimum detectable partial pressure for nitrogen to be 4×10^{-9} N/m^2 and the resolving power (10% valley definition) to be 44. Additional switch positions made possible the detection of masses 2, 3 and 4, but without scanning. The filament, which was rhenium, was always turned on at least one hour before critical measurements were to be made to ensure stability. Experience gained over the course of the project showed that the mass spectrometer performed well following the high temperature bake-outs and before mercury was admitted to the system, with well-resolved peaks being obtained for nitrogen, argon, water vapor, carbon dioxide, neon, helium and hydrogen. The sensitivity varied with the magnet used. For most of the runs, the sum of the partial pressures was between 50 to 75% of the corrected total pressure determined with the ionization gauge. Thus, the mass spectrometer was useful for semi-quantitative determinations of the background pressure of the gases in the system and for showing that the system was free from any detectable quantity of oxygen.

While the performance of the mass spectrometer towards the gases and vapors other than mercury did not change significantly once a satisfactory magnet had been obtained, its performance towards mercury changed markedly with time. As a result, reliance was placed on the ionization gauge for the mercury pressure measurements, while the main function of the mass spectrometer was to monitor the partial pressures of the other species to ensure that they remained so low as to be negligible with respect to the mercury pressures which were usually in the 10^{-4} to 10^{-2} N/m^2 range. In a few cases where the measured pressure was in the 10^{-5} N/m^2 range, the mass spectrometer readings were used to provide a small correction to the ionization gauge readings to obtain the mercury pressure.

Measurement of Vapor Pressures and Evaporation Rates

Most of the measurements were comparative rather than absolute. The principle used is illustrated in the sketch on the following page.

If a vapor pressure measurement was to be made, the evaporation chamber was held at a constant temperature and valve V1 was fully opened so that mercury vapor from the chamber could be leaked into the manifold leading to the gauges and pump through the smaller orifice, O1. The diameter of O1 was such that the pressure at the gauges when the pressure of mercury vapor in the chamber was 2.7×10^{-1} N/m^2 was about 1.3×10^{-5} N/m^2, while orifice O2 gave a similar pressure at the gauges when the pressure in the chamber was in the 10^{-3} N/m^2 range. The dimensions of the orifices were O1

(diameter, 0.0134 cm; length, 0.119 cm) and 02 (diameter, 0.0980 cm; length, 0.107 cm) and the ratio of their conductances as calculated from the expression (4):

$$F = K \cdot A \cdot V_a/4 \qquad (4)$$

where F is the conductance, K a factor determined by Clausing (see p. 94 of ref. 4) which depends on the length to radius ratio, A the orifice area and V_a the average velocity of the gas molecules, was 210. This value was used in intercomparing measurements through the two orifices. The calibration of the system for pressure measurements is described in connection with the measurements on pure mercury and in the Discussion section.

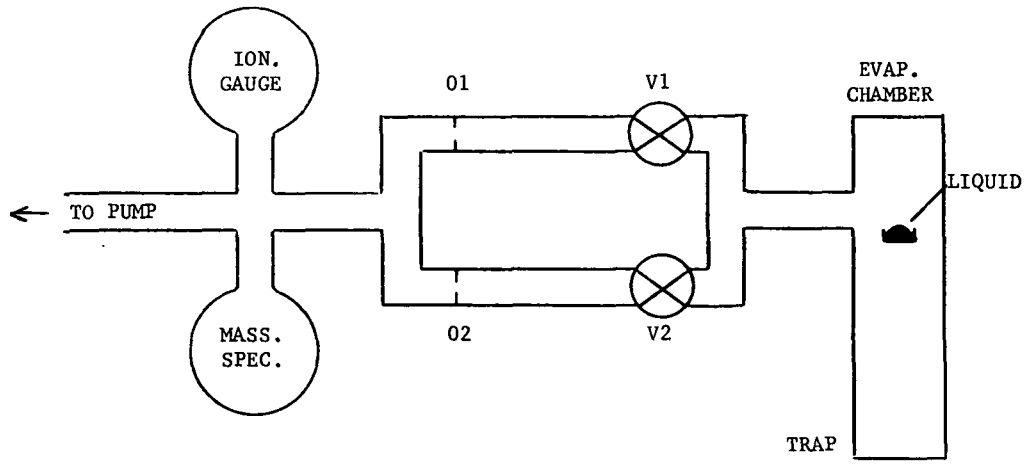

Since the conductances of the various portions of the system were held constant throughout the series of experiments, the pressures measured on the downstream side of 01 or 02 were proportional to the pressures on the up-stream side, provided sufficient time was taken for a steady state to be achieved. The time taken to reach the steady state was certainly less than 10 minutes and probably less than 1 minute, but about 20 minutes was usually allowed before taking readings. By taking measurements with mercury in the apparatus at a known temperature, the pressure of vapor in the apparatus could be calculated from the published vapor pressure data and the system could be calibrated for absolute pressure measurements.

For measurements of evaporation rates, the trap of the evaporation chamber was surrounded by liquid nitrogen so that the vapor evaporating from the amalgam or pure mercury was pumped away at high speed. This pumping action effectively lowered the pressure of vapor above the mercury surface and hence lowered the pressure on the up-stream sides of the orifices to the pressure gauges. The pressure on the up-stream side of the orifices 01 and 02 when valves V1 or V2 were fully open was governed by the rate of

evaporation of mercury from the amalgam and by the effective pumping speed of the refrigerated trap. Provided the pumping speed was held constant, the pressure recorded by the gauges depended only on the rate of evaporation of the mercury. Since the rate of evaporation of pure mercury can be calculated from its vapor pressure and equations (2) and (3), the rates of evaporation of the amalgams could be determined in absolute units.

Temperature Control and Measurement

For calibration of the system for absolute pressure measurements using the saturated vapor pressure of mercury as the standard, the system containing mercury was allowed to achieve temperature equilibrium with the laboratory. The laboratory temperature was measured with a mercury-in-glass thermometer which, like all thermometers used in this work, had been checked against a certificated thermometer with a calibration traceable to the National Bureau of Standards. The temperature of the mercury or amalgam was estimated to be correct to within 0.25°C.

For the evaporation rate measurements, the portion of the evaporation chamber surrounding the evaporation tube was wrapped with six turns of rubber hose of semicircular cross-section, three above and three below the evaporation tube, through which water at a constant temperature could be circulated (see Figure 4). In addition, for all except the first pure mercury experiment, three auxiliary electrical heaters in series with variable potentiometers were wound on the main body of the chamber and on the side arms to make possible more precise control of the wall temperature at the point at which the evaporation tube passed through the wall. Five copper-constantan thermocouples were attached to the glass close to the point of entry of the tube into the evaporation chamber to determine whether there were any significant heat leaks which might cause the temperature at this point to be different from the general wall temperature, and to help define the temperature as precisely as possible. The common reference junction for the thermocouples was attached to the bulb of the calibrated mercury-in-glass thermometer in the constant temperature water bath used for the general temperature control of the evaporation chamber. The thermocouple output was determined with a moving coil galvonometer. The water bath temperature could be determined to within ±0.1°C and the temperature difference between the bath and the other thermocouple junctions could also be determined to within ±0.1°C. The probable error in the determination of the thermocouple temperatures was therefore estimated to be about ±0.15°C.

In general, it was found that the four thermocouples closest to the point of entry of the evaporation tube indicated a temperature spread of about 0.5°C at 25°C and about 1°C at 55°C. The temperature of the point of entry was then taken as the average of the four readings. The error in this temperature could not be estimated very precisely. However, it was not considered possible for the temperature to lie outside the range indicated by the four thermocouples and, on this basis alone, the maximum possible error was judged to be no greater than about ±0.5°C. Since the symmetry of the placement of the thermocouples about the point of entry

should have caused the probable error to be about zero, it was concluded that the actual error was unlikely to exceed ±0.25°C, the average of the most probable error and the maximum possible error. The calculated temperature of the point of entry was used in the calculation of the temperature of the mercury or amalgam at the evaporation surface as described in Appendix IV.

MEASUREMENTS ON PURE MERCURY

The apparatus used in the study of pure mercury was as described in the previous section, except that only the smaller orifice 01 was provided as a leak to the pressure gauges. As mentioned, the pressure in the system after a 24 hour bake-out at 250°C prior to the introduction of mercury was variously indicated as 2.1×10^{-6} N/m^2 (ionization gauge), 5.7×10^{-7} N/m^2 (mass spectrometer, total of partial pressures), and 2.7×10^{-7} N/m^2 (ion pump), and the leak rate as measured with the ionization gauge was 7×10^{-15} moles.sec^{-1}. At no time during the experiments, except when it was intentionally admitted, was oxygen detectable in the system ($< 10^{-8}$ N/m^2).

The mercury used was of the highest purity commercially available. (Information on the sources and specifications of the mercury and the metals used in preparing the amalgams is given in Appendix II).

Measurements

After the double distillation of the mercury in the oxygen-free environment of the vacuum system, the mercury was allowed to return to room temperature and the evaporation tube was filled. The saturated mercury vapor was then allowed to leak through the orifice into the evacuated manifold connected to the pressure gauges. The steady gauge readings were recorded to provide a calibration factor relating the readings taken through 01 to the known saturation vapor pressure of the mercury at the measured room temperature. (Further calibration data for the orifices were obtained during the amalgam studies; the data for orifice 02 is summarized in Table 10.)

Following the measurement on the saturated vapor, liquid nitrogen was placed around the trap of the evaporation chamber and a well-formed meniscus about 0.15 cm high was produced above the horizontal surface of the evaporation tube. The base of the meniscus was bounded by the elliptical opening in the evaporation tube. This was the case for all the measurements on pure mercury and for most of the amalgams (see next section). The meniscus height was measured with a cathetometer and the meniscus area was calculated from the height as described in Appendix III. With the temperature of the point of entry of the evaporation tube into the evaporation chamber held constant at 25°C, pressure measurements were made through orifice 01 with both the ionization gauge and the mass spectrometer. The time allowed for temperature stabilization of the meniscus after adjustment of the temperature was 90 minutes. Subsequent observations showed that the time taken for stabilization was less than 30 minutes. After the measurements at 25°C

were completed, the temperature was raised to 40°C, the meniscus height and the liquid nitrogen levels were adjusted, and pressure measurements were made after allowing the usual 90-minute period for temperature stabilization. The procedure was repeated at about 55°C and 25°C to complete the measurements on the as-prepared mercury. The raw data is tabulated under the heading Run 1 in Table 2.

Run 2 was a repeat of Run 1 after the surface of the mercury exposed above the level of the evaporation tube had been cleaned by repeated sweepings. The sweepings physically dislodged drops of mercury which fell into the bottom of the liquid nitrogen trap. Any small drops which clung to the underside of the evaporation tube were allowed to evaporate before any further measurements were made. Pressures recorded during the sweeping process indicated very rapid responses of the gauges to movements of the sweeping blade.

At the end of Run 2, the system was closed off from the pump, the meniscus level was adjusted, and pure oxygen at a pressure of 240 N/m^2 was let in from an auxiliary vacuum system through a liquid nitrogen trap connected to valve 5 (Figure 2). Valve 5 was then closed and the oxygen was allowed to remain in the system for 70 minutes before being pumped out. When oxygen was no longer detectable and the pressure of gases and vapors other than mercury, as indicated by the mass spectrometer, had fallen to 1.3×10^{-6} N/m^2, Run 3 was begun. In Run 3, the sequence of measurements was as for Runs 1 and 2.

The last run for the pure mercury, Run 4, was carried out after repeatedly sweeping the mercury surface above the evaporation tube to remove any products which might have been formed at the surface as a result of the exposure to oxygen. The raw data for these first measurements on pure mercury are shown in the three left hand colums of Table 2. Some additional measurements on pure mercury made at the end of the program are reported later with the data for the amalgams (see next section).

The raw data was subsequently reduced to obtain the quantities in the three right hand columns of Table 2. The quantities are the meniscus area A, the meniscus temperature T, and the relative rate of evaporation per unit area. As mentioned previously, the area A was calculated from the meniscus height, the meniscus temperature was calculated from the relative evaporation rate as indicated by the ionization gauge and the measured temperature of the evaporation chamber wall as described in Appendix IV, and the relative evaporation rate per unit area was calculated as the (quotient of the ionization gauge reading divided by the area) $\times 10^7$.

The data in the two right hand columns of Table 2 are plotted in Figure 5 in the form of an Arrhenius plot of log (relative evaporation rate per unit area) versus 1/T°K. The best straight line through the points was fitted by linear regression. The standard error of estimate (SEE) is indicated on the figure. The slope of the regression line was used to calculate the heat of vaporization of the mercury. The value obtained was 58.8 kjoules·$mole^{-1}$ which may be compared with the literature value of 61.5 kjoules·$mole^{-1}$ (3).

The main conclusions to be drawn from the data of Table 2 and Figure 5 are:

a. The apparatus performed satisfactorily in that it was able to detect the changes in evaporation rate which accompanied changes in the temperature of the mercury. Further, the changes in rate were consistent with the known heat of vaporization of mercury;

b. The rate of evaporation of the mercury was not changed significantly by a 70-minute exposure to a 240 N/m^2 pressure of oxygen.

The results for the pure mercury provided data with which to compare the results for the amalgams discussed in the next section. They will also be referred to again in the Discussion section of this report.

MEASUREMENTS ON AMALGAMS

The studies of the tin, sodium and lithium amalgams followed the same general plan as for the pure mercury. Before each study, the glass portion of the apparatus had to be dismantled for cleaning and rebuilt with any necessary modifications. Those parts of the glassware, such as the evaporation chamber, which had to be reused, were washed with concentrated nitric acid to remove any residual mercury and then rinsed thoroughly with distilled water and dried before being reattached to the system. Other parts were completely replaced with new glass. Differences in the details of the apparatus between the experiments with the various amalgams will be mentioned in connection with the individual experiments.

Common features of all the experiments were that the equipment was always thoroughly leak tested before the introduction of mercury by enclosing it in a large plastic bag filled with helium and monitoring the system with the mass spectrometer. When the system had been shown to be free from external leaks, it was baked out for at least 7 hours with the maximum temperature being at least 190°C. On cooling, the leak rate was determined with the system closed off from the pump. At worst, the leak rate was 1.4×10^{-14} moles.sec^{-1}. If the leak rate for oxygen had been 25% of this figure, it would have taken about 4 days to supply enough oxygen to form a close-packed layer of oxygen atoms on a 1 cm^2 area of surface. However, using the mass spectrometer, no oxygen was detected in the system during the measurements except following the oxygen treatment of the surfaces at the start of Run 3; thus the oxygen pressure was less than 10^{-8} N/m^2. The system was always pumped down to a pressure of less than 1.3×10^{-6} N/m^2 as indicated by the ionization gauge before starting to prepare the amalgam.

Due to their different characteristics, different precautions against contamination were taken in handling the tin, sodium and lithium. In the case of the tin, the only precautions were to carry out the loading of the tantalum evaporation boat in the minimum of time and without direct handling

of the material. The sodium, which had been obtained in a 5 g quantity in a sealed glass capsule containing argon was able to be transferred to smaller capsules and sealed into them under vacuum without exposure to air. One of the smaller capsules, which was provided with a break seal, was connected to the main apparatus for the sodium amalgam experiments and was opened directly into the apparatus after it had been evacuated. The lithium, which had been obtained in foil form packed in a screw top jar with an argon atmosphere, was handled in dry nitrogen when loading the tantalum evaporation boat. Later observations indicated that some reaction had taken place between the foil and the nitrogen and that argon would have been a better choice of environment. This will be mentioned further in the description of the lithium amalgam study.

The mercury for preparing an amalgam was always outgassed by refluxing under vacuum and then sealed off while still hot. It was then opened to the system through a break seal and distilled once before evaporation of the other metal. After the other metal had been evaporated, the mercury was distilled a second time and used to dissolve the metal to make the amalgam.

The procedures for analyzing the amalgams are described in Appendix V. Essentially, the amalgams were first extracted with acid to separate the trace metal from the mercury and the aqueous extracts were then analyzed by atomic absorption spectrophotometry. The results were used to calculate the concentration of the trace metal in the amalgam.

1. Tin Amalgam

Apparatus - The apparatus used for the tin amalgam experiments was similar to that used for the measurements with pure mercury (Figure 3). The main changes were:

- provision was made for the evaporation of tin in flask F3 by the inclusion of the flange joint and electrical feed-through carrying a tantalum boat filled with about 0.5 g of tin;

- a glass-enclosed iron stirrer slug was placed in flask F3 to provide for magnetic stirring of the amalgam as it was formed;

- small, individually controlled electrical heaters were wound around the evaporation chamber and side-arms close to the level of the evaporation surface to minimize stray heat leaks to the evaporation surface; thermocouples to monitor the temperature at five critical points on the chamber walls were provided (Figure 4);

- the larger orifice, orifice 02, was placed in the system at the flange on the downstream side of valve 2 (Figure 2).

The last two of these modifications were made to improve the precision of temperature measurements at the point of entry of the evaporation tube into the evaporation chamber and to improve the precision of rate of

evaporation measurements by increasing the pressures to be measured in the manifold by a factor of about 200. The exact value of the factor turned out to be 210.

Amalgam Preparation - While the first distillation of the mercury was in progress, and throughout the amalgam preparation, the lower end of the evaporation chamber was surrounded with liquid nitrogen to protect the pump and pressure gauges from mercury vapor. After the distillation, the tin was evaporated onto the walls of F3 (Figure 3) by heating the tantalum boat to a white heat for consecutive three minute periods for a total of 30 minutes with an applied voltage of 26 volts. Finally, after it was judged that all the tin had evaporated, mercury was distilled into F3 until about 15cc had overflowed into R. The amalgam collected in R was sampled at A and analyzed as described in Appendix V. The concentration of tin was found to be only 100 ppm. The magnetic stirrer was then used to raise drops of amalgam from the pool in F3 up the walls to enrich them with tin and then guide them back to the pool. This process was continued until almost all of the tin had been removed from the walls and then more mercury was distilled to carry the enriched amalgam into R. When a sufficient volume of amalgam had been collected in R and when it was clear that further distillation would only result in dilution of the amalgam, analysis showed the tin concentration to be 53 ppm. Although this was much below the 200 ppm aimed for, the concentration was judged to be high enough for a meaningful experiment to be made in accord with the technical objectives. A duplicate analysis on a separate sample of the amalgam gave 51.5 ppm and confirmed the original analysis. (The reason for the low concentration of tin was not established with certainty. However, about 0.4 g of tin was found remaining in the tantalum boat at the end of the experiment. Since this was distributed over the tantalum, it may have reduced the resistivity of the boat and lowered the boat temperature so that the evaporation rate fell below the rate determined in preliminary tests.)

A portion of the amalgam was transfered to the evaporation tube using the scoop in T1 (Figure 3). The ball joint valve to the evaporation chamber was then closed to isolate the amalgam reservoir from the chamber in preparation for the measurements.

Measurements - The evaporation rate measurements on the tin amalgam were made by the same procedure and in the same sequence as for the pure mercury. The results are given in Table 3 together with derived quantities obtained using the corrections for the temperature and area of the evaporation surface as described in Appendices III and IV. Although the rates of evaporation of the amalgam were much reduced by the exposure to oxygen at the start of Run 3, there was no change in its clean, bright appearance at the evaporation surface.

The data of Table 3 is plotted as the logarithm of the relative evaporation rate per unit area against 1/T°K in Figure 6. The best straight line through all the points for the clean surfaces (Runs 1, 2 and 4) and the best straight line through the points for Run 3 (oxygen-treated surface) were

fitted by linear regression. They are shown by the solid lines in the figure while the broken line is the regression line from the data for pure mercury, Figure 5.

The main conclusions to be drawn from the data of Table 3 and Figure 6 are:

a. The rate of evaporation from the clean surface of a 52 ppm tin amalgam is similar to the rate for pure mercury;

b. Since the rate of evaporation of the 52 ppm tin amalgam was similar to that for pure mercury, its vapor pressure was also similar to that for pure mercury.

c. The rate of evaporation of a 52 ppm tin amalgam at 25°C is reduced by at least 80% by exposure to a 290 N/m^2 pressure of oxygen for 70 minutes; the reduction in rate appears to be due to an insoluble surface film.

d. The effect of the oxygen exposure on the rate of evaporation can be completely removed by mechanical cleaning of the surface.

The results for the tin amalgam will be compared with the results for the other amalgams and pure mercury in the Discussion section.

2. Sodium Amalgam

Apparatus - As a result of the experience gained in preparing the tin amalgam, and in view of the greater ease of evaporation of sodium, the apparatus used for the sodium amalgam study was as shown in Figure 7. This retained the main features of the earlier apparatus but included some modifications:

- the sodium was mounted in a sealed glass capsule at the end of an inverted U so that the evaporation could be carried out by external electrical heating;

- the use of two interconnected sloping manifolds, each with a magnetically operated scoop, made possible a greater degree of control over the amalgam concentration by giving more options for concentration and dilution than the previous design;

- a magnetically operated ball joint valve at the amalgam manifold end of the evaporation tube was provided to prevent evaporation; thus volumetric measurements could be made on the mercury in the tube to obtain independent measurements of the rates of evaporation;

- a U-tube trap of large bore was included in the pumping line between the amalgam manifold and the top of the evaporation chamber to avoid the need to use the evaporation chamber trap for protection of the pump and gauges during amalgam preparation;

• a by-pass line L was provided to make possible the introduction of pure mercury into the evaporation tube if it should be decided to make measurements on pure mercury at the end of the study of sodium amalgam.

Amalgam Preparation - The steps in making the sodium amalgam were sufficiently different from those for the other amalgams to require a separate description. After the mercury had been distilled into flask F2 (Figure 7) and seal S2 had been closed, the break seal BS2 was opened and the inverted U containing about 0.5 g of sodium was heated to 400°C for 7 hours using a tubular electric furnace. When it was judged that enough sodium had been distilled into R1, seal S3 was closed. At the end of the distillation, the glass in the U was dark brown, almost black, due to attack by the sodium.

The distillation of mercury from F2 into R1 was begun. The first drops of mercury to come into contact with the sodium evaporated almost explosively due to the large amount of heat liberated by the amalgamation. Subsequently, an irregular mass of solid amalgam was formed which only dissolved slowly in the mercury which was added later. When analysis showed that an amalgam of about 1000 ppm had been produced in R1, nine scoopfuls of it were transferred to R2 and S4 was sealed off. The amalgam in R2 was repeatedly diluted by mercury distilled from F2, stirred with the scoop, sampled and analyzed (see Appendix V) until it was decided that no further improvement in composition was needed. The analysis of the amalgam showed it to contain 229 ppm of sodium. The amalgam in R2 was sampled again at the end of the sodium amalgam study. The sodium content was found to be 228 ppm. It was noticed that the clean amalgam had a contact angle very close to 90° against the glass in the air-free, mercury vapor environment inside the system.

Finally, enough of the 229 ppm sodium amalgam was transferred to the evaporation tube to give a well-formed meniscus at the evaporation surface and both ball joint valves were closed.

Measurements - The evaporation rate measurements on the sodium amalgam were carried out in the same sequence as for the pure mercury and the tin amalgam. However, an important addition was that volumetric measurements to obtain absolute evaporation rates were carried out concurrently with some measurements based on pressure readings. In the volumetric measurements, the cathetometer was used to determine the positions and shapes of the menisci at both ends of the evaporation tube. From these observations, the mean evaporation rates over specific time periods were calculated. The results from the pressure measurements are shown in Table 4 together with the quantities derived using the corrections for the temperature and area of the evaporation surface (Appendices III and IV) while the volumetric rate measurements are given in Table 5.

In the experiment with oxygen (Run 3), it was established from pressure measurements at the beginning and end that only a small proportion of the oxygen let into the system at a pressure of 240 N/m^2 had reacted during the 70 minute exposure. This was shown by opening the system momentarily to the McLeod gauge of the auxiliary vacuum system at the end of the 70 minute

period. The pressure, which could be determined to the nearest 13 N/m^2 was 215 N/m^2 -- a decrease of about 26 N/m^2 from the initial pressure. Since the volume of the apparatus was about 5 l, a drop of 26 N/m^2 in the pressure would correspond to the removal of about 6×10^{-5} moles or 2 mg of oxygen from the gas phase. This quantity is an upper limit since about one fifth of the observed pressure drop was due to expansion into the approximately 100 cc volume of the evacuated manifold of the auxilliary system. Unlike the tin amalgam, the sodium amalgam showed definite signs of reaction with the oxygen. These were first noticeable on the large exposed surfaces of the amalgam in R1 and R2 but not on the exposed meniscus in the evaporation tube. The appearance of these surfaces was, at first, as though they were covered with very slender, transparent needles radiating from the scoops and the other glass surfaces. Later observations suggested that the appearance was caused by folds in a very thin surface film, the folds being very straight and roughly parallel so as to give the illusion of closely-packed needles. The films could be easily swept aside by moving the scoops which then became covered with a layer of silvery material with a matte appearance, presumably consisting of the surface film and trapped amalgam. The appearance of the evaporation surface was, at first, less obviously affected by the oxygen exposure. The meniscus still appeared smooth and bright to the naked eye though, when viewed through the cathetometer telescope, a reflected beam of light from a remote source (flashlight) in the equatorial plane showed a more distinct halo than was usual for clean amalgam surfaces. This suggested increased light scattering from the surface, possibly due to the presence of small particles or a surface film. The halo became still more pronounced toward the end of Run 3 as the volume of the meniscus diminished due to evaporation and to thermal contraction of the mercury in the evaporation tube on cooling the evaporation chamber from 55° to 25°C. At the end, the meniscus was no longer smooth and bright even to the naked eye but showed an appearance as though it were enclosed in a very thin, crinkled, transparent membrane. At this point, the shape of the meniscus was that of a disc with slightly rounded corners -- a shape quite unlike that shown by the free surface of the amalgam when clean.

Another observation made for the sodium amalgam was that the tendency for drops to cling to the underside of the evaporation tube after sweeping of the surface appeared to be greater than for pure mercury and the tin amalgam. This was the case both before and after the oxygen exposure. For pure mercury, any drops which clung to the tube evaporated quite quickly so, provided sufficient time was allowed for their evaporation, there was no concern about their effect on the measured rates. In the case of the sodium amalgam, the drops also evaporated quite quickly but they left a small solid residue, presumably of a solid amalgam of low vapor pressure, on the underside of the tube. That these residues were of no significance in affecting the measurements was concluded from the following considerations. Before evaporation, the largest of the drops was roughly spherical and about 0.1 cm in diameter. The surface area of such a drop would have been about 0.008 cm^2 as compared with the 0.2 to 0.3 cm^2 area of the meniscus. Thus, on the basis of its original exposed area, it would have contributed no more than 4% to the total evaporation rate. However, because it was allowed to

evaporate to a solid residue before evaporation rate measurements were taken, its contribution would have been negligible both because of its small volume and area and because of the reduction in vapor pressure brought about by the increased sodium concentration. Although the volume of the irregular solid residue was difficult to assess in precise terms, it was clearly very small. If its composition was that of the most dilute sodium amalgam which exists as a solid at 25°C (about 0.3% Na (21)), its volume would have been less than one tenth of the volume of the original 229 ppm drop, say about 5×10^{-5} cc as compared with 5×10^{-4} cc for a 0.1 cm diameter drop. As will be seen from the results of the volumetric measurements on the evaporation of sodium amalgam, this volume of mercury would evaporate from 0.25 cm^2 area of a clean meniscus of the amalgam at 25° in about 10 seconds.

The logarithms of the relative evaporation rates per unit area are plotted against 1/T°K in Figure 8. The regression lines through the points for Runs 1, 2 and 4 (clean surface) and Run 3 (oxygen-treated surface) are shown as full lines while the broken line is the regression line from the data for pure mercury, Figure 5. The data from the volumetric measurements will be discussed at greater length in the Discussion section.

From the results shown in Tables 4 and 5 and Figure 8, it was concluded that:

a. The rate of evaporation from the clean surface of a 229 ppm sodium amalgam is similar to the rate for pure mercury;

b. Since the rate of evaporation of the amalgam was similar to the rate for pure mercury, its vapor pressure was similar to that for pure mercury;

c. The rate of evaporation of the amalgam was reduced by at least 97% over the 25° to 55°C temperature range by a 70 minute exposure to a 240 N/m^2 pressure of oxygen; the reduction in rate appeared to be due to the formation of an insoluble surface film;

d. The effect of the oxygen exposure on the rate of evaporation of the amalgam can be completely removed by mechanical cleaning of the surface.

The results for the sodium amalgam will be considered further and compared with the results for the other amalgams and pure mercury in the Discussion section.

3. Lithium Amalgam

Apparatus - The apparatus used for the experiments with lithium amalgam combined features of the apparatus used in the experiments with the tin and sodium amalgams. The lithium was evaporated from a tantalum boat in the same flask as used for the tin (Figure 3). The manifold for the preparation

of the lithium amalgam was also as in Figure 3 though a connection was provided to make possible the distillation of pure mercury into the evaporation tube at the end of the amalgam experiment; this feature was as L in Figure 7 but with a spare break seal being included in the connection in case a need should develop to provide entry to the system without breaking the vacuum. The rest of the apparatus was as for the sodium amalgam measurements including the U-tube trap between the amalgam manifold and the top of the evaporation chamber, and the ball joint valve at the manifold end of the evaporation tube.

The pure lithium (see Appendix II), which was in the form of foil was handled in a glove bag filled with dry nitrogen. The foil was sliced with cleaned stainless steel scissors and about 0.3 g was packed into the tantalum boat which was then quickly mounted in the evaporation flask and the system, which had been flushed with dry nitrogen, was pumped out.

Amalgam Preparation - The procedure for making the lithium amalgam was as for the tin amalgam though the temperature needed for evaporation of the lithium was about 500°C lower. During the lithium evaporation, the glass of the evaporation flask darkened to black due to attack by the hot metal. Then, when the mercury was distilled into the flask to form the amalgam, it was noticed that the amalgam had a dull surface. This appeared to be due to some insoluble dark material floating on it. The two most likely sources for this material were the black reaction product between the lithium and the borosilicate evaporation flask, and lithium nitride (Li_3N) formed before the lithium was put into the system. Later observations seemed to confirm that both lithium nitride and some other material were present. Thus, small bubbles of nitrogen were liberated from the amalgam for some while, apparently due to reaction between lithium nitride and the glass walls. (The existence of such a reaction was subsequently confirmed (22).) When the liberation of nitrogen had stopped and a satisfactorily low pressure of less than 1.3×10^{-6} N/m^2 obtained, some dark material still remained on the amalgam surface. This was believed to be the product of the reaction between lithium and the glass. The final concentration of lithium in the amalgam was found to be 165 ppm. A confirmatory analysis of amalgam taken from the reservoir at the end of the experiment also showed the concentration to be 165 ppm. The analyses did not seem to be affected by the insoluble material on the amalgam surface since this clung to the walls so that little of it was transferred.

When the amalgam concentration was judged satisfactory, amalgam was transferred to the evaporation tube in readiness for the evaporation measurements. It was noted that the evaporation surface was clean and bright.

Measurements - The evaporation rate measurements for the lithium amalgam were carried out in the same sequence as for the other amalgams. The results are shown in Table 6, together with the quantities obtained by applying the corrections for the temperature and area of the evaporation surface (Appendices III and IV).

As for the sodium amalgam, pressure measurements made at the beginning and end showed that only a small portion of the oxygen let into the system at the start of Run 3 could have reacted with the amalgam, during the 70 minute exposure. The initial oxygen pressure was 300 N/m^2 and the final pressure, 280 N/m^2. This set an upper limit of about 3×10^{-5} moles or 1 mg on the quantity of oxygen removed from the gas phase during the exposure to the amalgam. Also, during the evaporation rate measurements following the oxygen exposure, the meniscus behaved very much like the meniscus of the sodium amalgam in that, at first it appeared clean and bright but later, as the meniscus volume became smaller, the surface appeared to be enclosed in a thin, wrinkled, transparent membrane and the meniscus shape approximated that of a disc with rounded edges. An important observation was that, as the temperature was increased from 40° to 55°C, thermal expansion of the amalgam in the evaporation tube caused the meniscus to become so large that part of it broke away and fell into the trap. In spite of the damage this must have caused to the film on the amalgam surface, no increase in the evaporation rate above that which would have been expected from the data for oxygen-treated surfaces at 25° and 40° was observed (see Figure 9).

The logarithms of the relative evaporation rates per unit area of Table 6 are plotted against 1/T°K in Figure 10. The full lines drawn through the points for Runs 1, 2 and 4 (clean surface) and Run 3 (oxygen-treated surface) were fitted by linear regression and the broken line is the regression line from the data for pure mercury, Figure 5.

From the data on the 165 ppm lithium amalgam, it was concluded that:

a. The rate of evaporation from the clean surface of the amalgam is similar to the rate for pure mercury;

b. Since the rate of evaporation of the amalgam was similar to the rate for pure mercury, its vapor pressure was similar to that for pure mercury;

c. The rate of evaporation of the amalgam was reduced by at least 93% over the 25° to 55°C temperature range by a 70 minute exposure to a 300 N/m^2 pressure of oxygen; the reduction in rate appears to be due to the formation of an insoluble surface film;

d. The surface film has some ability to heal if broken;

e. The effect of the oxygen exposure on the rate of evaporation of the amalgam can be completely removed by mechanical cleaning of the surface.

The results for the lithium and other amalgams will be discussed further and compared with those for mercury in the Discussion section.

4. Final Measurements on Mercury

At the end of the measurements on the lithium amalgam, mercury was distilled so as to run into the evaporation tube and wash out the amalgam. The volume of the tube was estimated to be 5 cc and 50 cc of mercury was distilled to flush it out and replace the amalgam with essentially pure mercury. A set of measurements was then made on the mercury to provide a final check on the system performance. These measurements were made using orifice 02 whereas the original measurements had been made using orifice 01. The analysis of the mercury at the end of the run showed it to contain 0.3 ppm of lithium. This is considered to be an upper limit on the lithium content since it was believed to have been contaminated during removal from the evaporation tube. The results are recorded in Table 7 and they are plotted in the usual form of log (relative evaporation rate per unit area) versus 1/T°K in Figure 11. The regression line for this data is the solid line in the figure while the line for the original set of data on pure mercury is shown by the broken line. While the results confirmed that no catastrophic change had occurred in the performance of the system, they suggested that a change in the sensitivity of the ionization gauge might have occurred during the course of the program. This possibility is discussed in the next section in connection with the magnitudes of the errors and the general significance of the data.

GENERAL DISCUSSION

Relative Evaporation Rates

The evaporation rate data for pure mercury and the amalgams were given in arbitrary units in Tables 2, 3, 4, 6 and 7, and in Figures 5, 6, 8, 10 and 11. The regression lines fitted to the log (evaporation rate/unit area) versus 1/T°K plots for the clean surfaces of pure mercury and the amalgams and for the oxygen-treated surfaces are shown again in the composite plot of Figure 12. The average standard error of estimate (SEE) for the points represented by the regression lines is shown in the figure. Attention must be drawn immediately to the difference of about 0.2 units on the log scale between the positions of the regression lines for the first and last sets of data for mercury. This difference, the value of which may be calculated from the equations of Table 9 to be 0.196 at 40°C, is much larger than the average standard error of estimate for the regression lines (0.074 log units) and it represents an apparent reduction of almost 40% in the relative evaporation rates per unit area from the first run to the last. This suggests that there was a reduction of almost 40% in the ionization gauge sensitivity over the course of the program since an analysis of likely errors (summarized in Table 8) does not lead to any other explanation. Additional facts which are consistent with the idea that there was a systematic downward drift in the ionization gauge sensitivity are:

a. The data for the last points (Run 4) in each of Tables 2, 3 and 6, and the associated Figures 5, 6 and 10, tend to lie below the corresponding points (Runs 1 and 2) obtained earlier; (while the same trend is not apparent for the sodium amalgam data of Table 4 and Figure 8, there is reason for believing it to be masked by larger than usual errors in two of the points for Run 1).

b. The standard errors of estimate are about twice as large as would be expected from the combined random errors indicated in Table 8; the unexpectedly high SEE's could be attributable to a systematic error from a drift in gauge sensitivity being superimposed upon the random error contribution to the SEE.

Since the presumptive evidence for a drift in ionization gauge sensitivity over the course of the measurements was strong, a correction for such a drift was made as follows. It was assumed that the drift had occurred at an essentially constant rate while the equipment was in use but that, for simplicity, the total drift could be considered to have taken place in steps from one experiment to the next. Then, to correct for the changes, the factors 1.1, 1.2, 1.3 and 1.4, respectively, were used to correct the ioniza-

tion gauge readings for the tin, sodium, and lithium amalgam experiments, and the last mercury experiment, for comparison with the first mercury experiment. The revised regression lines are plotted in Figure 13. While more sophisticated ways of correcting the gauge readings for the drift could have been used, (e.g., making a correction on the basis of hours of operation of the gauge in the presence of mercury), it was not felt that enough information was available to justify more than a simple empirical correction.

The important conclusion to be drawn from Figure 13 is that the evaporation rates for mercury and the clean amalgams all lie within the approximately 15% experimental error of each other while the rates of evaporation of the amalgams which have been exposed to oxygen are at least 90% lower at 25°C. It is now clear that the low rates of evaporation of tin, sodium and lithium amalgams observed in the earlier study (2) were presumably due to some form of contamination such as oxide, hydroxide or nitride.

In regard to the mechanism by which exposure to oxygen reduces the rate of evaporation of the amalgams, the evidence of the present study is that the reduced rates result from the formation of thin, insoluble films on the surfaces. The effects of the films, and presumably the films themselves, can be removed by mechanical sweeping of the surfaces. The fact that the film does not reform without further exposure to oxygen indicates that it is not sufficiently soluble to form a reservoir of dissolved material from which it can be regenerated by Gibbsian adsorption. While the films can be removed without difficulty, it is significant that on one occasion the surface film of the oxygen-treated lithium amalgam must have been broken by the breaking away of a drop of amalgam from the meniscus, without causing more than a momentary increase in the evaporation rate. Thus, at least for the lithium amalgam, the surface film does have some ability to heal if broken.

The retardation of evaporation by the films, which presumably consist of metal oxide, must be attributed to a low permeability of the films to the passage of mercury vapor. Depending on the structure of the oxide film, the mercury atoms may escape from the amalgam by either activated diffusion through pores of atomic dimensions in the film or by gas phase diffusion through pores with effective diameters large with respect to the diameter of the mercury atom. If the former, the apparent heat of vaporization of the mercury (which can be deduced from the slopes of the regression lines in Figure 13) should be increased over the value for pure mercury or for the clean surface of the amalgam. If the latter, the heat of vaporization should be unchanged. Of the three metals studied as amalgams, only tin appeared to show an increase in the heat of vaporization, whereas the other two appeared to show a decrease. The decrease in the heats for sodium and lithium are believed not to be real but to be due to disproportionately large errors in the low pressure readings resulting from residual mercury in the manifold following measurements at higher pressures. While this hypothesis has not been confirmed quantitatively, it was observed on several occasions that closing off of the glass system from the manifold following measurements on mercury showed that there was a small but detectable background pressure of mercury which could not be removed in any reasonable period of time. Errors

from this source would be expected to lead to an apparent reduction in the heat of vaporization which would be most significant when the measured pressures were lowest i.e., for the oxygen-treated amalgams. Thus, it is likely that the heats of vaporization of the oxygen-treated amalgams as determined from the lines in Figure 13 would be at least slightly underestimated. For this reason, it is not considered significant that the heats of vaporization of the oxygen-treated sodium and lithium amalgams appeared to be lower than the value for pure mercury, but it is considered significant that the heat for the oxygen-treated tin amalgam appeared to be raised above the value for pure mercury.

The differences in the rates of evaporation of the oxygen-treated amalgams may be due to several factors:

a. Differences in the concentrations of the metals in the amalgams

b. Different structures and thicknesses of the surface films.

It seems likely that the second of these will be the most important, provided enough metal is present to form a dense surface film and provided enough time is allowed for the film to grow to an adequate thickness. It is certain that there was enough trace metal in each of the amalgams of the present study to form oxide layers many atomic diameters thick. However, the rate of reaction of the tin amalgam with oxygen may have been lower than the rates for the other amalgams because of lower surface concentrations of tin; the lower surface concentrations would result from the lower bulk concentration of the tin amalgam and a probably lower adsorption of tin at the mercury surface (as indicated by the data of Semenchenko (12)). A lower rate of reaction would lead to a thinner film and, probably, a smaller effect on the retardation of evaporation.

Absolute Evaporation Rates in the Evaporation Chamber and in Free Space

With the exception of the volumetric measurements of the evaporation rates of the sodium amalgam (Table 5), all the rate data discussed has been presented in arbitrary units. Comparison of the volumetrically determined absolute evaporation rates for the sodium amalgam with the rates expressed in arbitrary units represented by ionization gauge readings gives a factor for converting all the rate data to absolute terms. This has been done in calculating the right hand ordinate scale of Figure 13. The relationship was found to be:

$$\text{Rate of evaporation (in g.cm}^{-2}\text{.sec}^{-1}\text{)} = \text{relative evaporation rate per unit area} \times 2.70 \times 10^{-6}$$

The absolute evaporation rates which are shown in Figure 13 apply to the specific conditions in the evaporation chamber when the flow of mercury vapor away from the evaporation surface is limited by the conductance of the tube leading to the trap. The evaporation rates in free space would be a little higher than the values of Figure 13 because conductance would not be a limiting factor.

There are two ways of determining the magnitude of the correction which should be applied to the evaporation rates of Figure 13 to obtain values for free space. The first recognizes that (i) the rate of evaporation is, as shown by equation (3), proportional to $(P_{sat}-P)$, where P_{sat} is the saturation vapor pressure of the mercury or amalgam and P is the effective pressure above the surface, and (ii) the rate of flow of vapor to the trap is proportional to P, since the effective pressure in the trap is negligible, and that P can be calculated for the evaporation chamber geometry for various temperatures and areas of the evaporation surface. Such calculations are described in Appendix VI. They indicate that P is likely to be less than $P_{sat}/15$. Thus, since it follows from equations (2) and (3) that the evaporation rate in free space G_{fs} should be related to the rate G_{ec} in the evaporation chamber by the relationship:

$$\frac{G_{fs}}{G_{ec}} = \frac{P_{sat}}{P_{sat}-P} \qquad (5)$$

then G_{fs} will lie between G_{ec} and $(15/14)G_{ec}$.

In the second method of approach to calculating G_{fs} from G_{ec}, P is determined experimentally and the measured value substituted in equation (5). If, as seems likely, P is essentially identical to the pressure above the evaporation surface which was monitored in the evaporation rate measurements, then P can be determined from the ionization gauge readings of the rate measurements (e.g. Tables 2, 3, 4, 6,and 7) if the calibration factor relating the gauge readings to the pressure in the chamber is known. This factor was determined from readings taken on various occasions when mercury in the system was allowed to come to equilibrium with its saturated vapor at the laboratory temperature. From the results summarized in Table 10, the calibration relationship was shown to be:

$$\text{Pressure } (N/m^2) = \text{Ionization Gauge Reading (torr)} \times 1.36 \times 10^4$$

Applying this relationship to the data from Tables 2, 3, 4, 6 and 7, values of P were obtained which could be combined with the known values of P_{sat} using equation (5) to calculate G_{fs} from the G_{ec} regression lines of Figure 13. As an example, G_{ec} was calculated to be 1.1×10^{-4} $g.cm^{-2}.sec^{-1}$ at 25°C while P above a 0.25 cm^2 evaporation surface at 25°C was found to be 1.3×10^{-2} N/m^2. Then, knowing that P_{sat} for mercury at 25.0°C is 2.76×10^{-1} N/m^2, application of equation (5) gave a value of 1.15×10^{-4} $g.cm^{-2}.sec^{-1}$ for G_{fs}. This may be compared with the value of G_{fs} (G_{esc}) calculated from the kinetic theory using equation (2) - 1.0×10^{-4} $g.cm^{-2}.sec^{-1}$. This agreement must be considered satisfactory when the previously discussed sources of error are taken into account. Thus, the treatment of the data for mercury is seen to lead to reasonable results for the rate of evaporation in free space.

The same approach was taken in calculating the rates of evaporation in free space (see Table 11) from the amalgam surfaces. However, some additional consideration was necessary to justify the choice of values of P_{sat} for the clean amalgams and for the oxygen-treated amalgams. For the clean amalgams, the similarities of their rates of evaporation to the rates of evaporation for mercury could only be explained if their P_{sat} values were similar to the P_{sat} values for mercury. Thus, referring to equation (3), it can be seen that if P is small, the P_{sat} values are essentially proportional to the G values.

The situation is different for the oxygen-treated surfaces. Here, definite differences in the evaporation rates from those for mercury do exist. However, since P_{sat} should not be changed by the physical presence of the surface film, and since the rate of diffusion away from the surface through the physical barrier provided by the film will be proportional to $(P_{sat}-P)$, equation (5) should still apply. It is upon this basis that the rates of evaporation in free space for all the oxygen-treated amalgams (Table 11) have been calculated. However, because the apparent heat of vaporization of the tin amalgam through the film is higher than for pure mercury, the true driving force for the rate determining step in the diffusion of mercury away from the surface must be somewhat less than $(P_{sat}-P)$. Thus, the rates of evaporation for the tin amalgam in free space after exposure to oxygen will have been slightly underestimated in Table 11.

CONCLUDING REMARKS

The work described in this report was stimulated by a need to know whether the low rates of evaporation previously observed for some dilute amalgams were due to insoluble films or to Gibbsian adsorbed layers. Whereas Gibbsian layers would have an inherent ability to reform if the surface were disturbed, insoluble films might not reform spontaneously. Thus, insoluble films would be less desirable than Gibbsian layers if Gibbsian layers could cause a large reduction in evaporation rate.

While the experiments described show conclusively that insoluble surface films formed by exposure of amalgams to oxygen can be removed by vigorous cleaning of the surface, there is evidence from the experiments with lithium amalgam that the films have some ability to heal. The extent of this ability should be investigated further if the use of mercury in space is still of interest. Also, whereas the films on the amalgams of the study reported here were formed by reaction with oxygen, films should also be able to be formed by interaction between amalgams and a variety of other gases (e.g. water vapor) or liquids (e.g. water, ethanol). The ability to form or renew surface films using other active species than oxygen could prove valuable in space applications.

SUMMARY OF RESULTS

Using an ultra-high vacuum apparatus designed for the purpose, pure mercury and dilute amalgams of tin, sodium and lithium were prepared in successive experiments. The amalgam concentrations were tin, 52 ppm; sodium, 229 ppm; and lithium, 165 ppm. The rates of evaporation of the mercury and the amalgams were determined at temperatures between 25° and 55°C both before and after a 70 minute exposure to about a 270 N/m^2 pressure of oxygen. In addition, the rates were determined again after the liquid metal surfaces had been cleaned by mechanical sweeping.

The results showed that:

1. The rates of evaporation of pure mercury and the amalgams were the same, within about a 15% experimental error, over the 25° to 55°C temperature range.

2. The rates of evaporation of the amalgams, but not of the mercury, were reduced by the exposure to oxygen; the reductions in the rates for the amalgams were at least 80% over the 25° to 55°C temperature range.

3. The reduced rates of evaporation, at least for the sodium and lithium amalgams, were caused by the formation of thin, transparent, insoluble oxide films which only became visible when they buckled as the surface area of the liquid was reduced; the films could be removed by sweeping the surface.

4. Although the effects of the oxygen treatment could be easily removed by sweeping the surface, there is evidence that the film on the oxygen-treated lithium amalgam had some ability to heal if broken in other ways. Thus, on one occasion it was observed that the breaking away of a drop from the large meniscus did not result in an increase in the rate of evaporation.

5. The rates of evaporation of pure mercury and the clean and oxygen-treated amalgams in free space were calculated for 25°, 40° and 55°C. The results were:

	Rates of evaporation in free space x 10^4 ($g.cm^{-2}.sec^{-1}$)		
	25°C	40°C	55°C
Pure mercury and clean amalgams	1.0	3.0	8.5
O_2-treated tin amalgam (52 ppm)	0.095	0.32	1.3
O_2-treated sodium amalgam (229 ppm)	0.025	0.048	0.088
O_2-treated lithium amalgam (165 ppm)	0.085	0.19	0.32

6. Since the rates of evaporation of the pure mercury and the clean amalgams were the same within the experimental error, their saturated vapor pressures must also have been the same within the experimental error.

REFERENCES

1. A. H. Ellison and S. B. Tejada, NASA CR72441, July 23, 1968.

2. A. M. Schwartz and S. B. Tejada, NASA CR72715, April 20, 1970.

3. G. T. Engel in Kirk-Othmer Encyclopedia of Chemical Technology, 2nd ed., Vol. 13, p. 218, Interscience, New York, 1967.

4. S. Dushman, Scientific Foundations of Vacuum Technique, 2nd ed., Wiley, New York, 1966.

5. K. K. Kelley, U. S. Bureau of Mines Bulletin No. 585, 1960, (reissue of Bull. No. 383, 1935).

6. N. K. Adam, The Physics and Chemistry of Surfaces, 3rd ed., Oxford University Press, London, 1941.

7. F. Sebba and E. K. Rideal, Trans. Faraday Soc., 37, 273 (1941).

8. N. L. Jarvis, C. O. Timmons and W. A. Zisman, in Retardation of Evaporation by Monolayers, ed. V. K. LaMer, p. 41, Academic Press, New York, 1962.

9. S. Glasstone, Textbook of Physical Chemistry, 2nd ed., Van Nostrand, New York, 1946.

10. F. E. Poindexter, Phys. Rev., 28, 208 (1926).

11. International Critical Tables, Vol. 3, p. 284, 1928.

12. J. H. Hildebrand, A. H. Foster and C. W. Beebe, J.A.C.S., 42, 545 (1920).

13. V. K. Semenchenko, Surface Phenomena in Metals and Alloys, Pergamon Press, New York, 1961.

14. R. Pohl and P. Pringsheim, Verh. deutsch. Phys. Ges., p. 431, 1931; as referenced in V. K. Semenchenko, Surface Phenomena in Metals and Alloys, p. 235, Pergamon Press, New York, 1961.

15. U. R. Evans, The Corrosion and Oxidation of Metals, St. Martin's Press, New York, 1960.

16. E. de B. Barnett and C. L. Wilson, Inorganic Chemistry, 2nd ed., Longmans, New York, 1957.

17. A. Feldman, Giorn. chim. ind. applicata., 9, 455 (1927); CA 22, 362 (1927).

18. C. Kemball, Proc. Roy. Soc. A201, 377 (1950).

19. R. D. Craig, in Modern Aspects of Mass Spectrometry, ed. R. I. Reed, p. 21, Plenum, New York, 1968.

20. G. McDonagh, Veeco Instrument Company, private communication.

21. International Critical Tables, Vol. 2, p. 436, 1927.

22. N. Smith, Foote Mineral Company, private communication.

23. J. R. Hutchins, III and R. V. Harrington, in Kirk-Othmer Encyclopedia of Chemical Technology, 2nd ed., Vol. 10, p. 533, Interscience, New York, 1966.

24. R. C. Weast (ed.), Handbook of Physics and Chemistry, 48th ed., 1967-1968, Chemical Rubber Company, Cleveland, 1967.

25. E. A. Moelwyn-Hughes, Physical Chemistry, p. 24, Pergamon Press, New York, 1957.

26. International Critical Tables, Vol. 4, p. 440, 1928.

27. S. N. Zadumkin and V. G. Egiev, Fiz. Metal. i Metalloved, 22, 121 (1966); CA 65, 17839h (1966).

TABLE 1

CHARACTERISTIC PROPERTIES OF THE METALS

Metal	Atomic Weight[a]	Atomic Radius[b] (Å)	Ionic Radius[b] (Å)	M. Pt.[a] (°C)	B. Pt.[a] (°C)	Heat of Vaporization[a] (kjoules·mole^{-1})	Surface Tension (dyne·cm^{-1}) γ^t(°C)
Hg	200.59	1.59	0.66 (II)[e]	-38.87	366	58.5	467 (60°)[c]
Sn	118.69	1.40	0.65 (IV)	231.89	2270	(230)	526 (253°)[c]
Na	22.99	1.86	1.012	97.81	892	98	222 (100°)[c]
Li	6.939	1.52	0.758	179	1317	136	398 (186°)[d]

a. ref (24)

b. ref (25)

c. ref (26)

d. ref (27)

e. Roman numerals denote valency states

TABLE 2

EVAPORATION RATE DATA FOR PURE MERCURY

	Wall Temp (°C)	IG[a] Reading x10^7 (torr)	Meniscus Height, h (cm)	Meniscus Temp, T (°C)	Meniscus Area A (cm^2)	Relative[b] Evap Rate per cm^2
Initial Measurements (Run 1)	25.0	12	0.12	23.6	0.24	48
	40.6	27	0.13	37.2	0.25	109
	55.0	59	0.085	47.7	0.22	269
	24.6	8.6	0.149	23.5	0.27	32
Surface Swept (Run 2)	24.6	8.6	0.107	23.5	0.23	37
	40.6	25	0.119	37.5	0.24	105
	55.5	48	0.077	49.5	0.21	230
Exposed to Oxygen at 240 N/m^2 for 70 minutes (Run 3)	25.1	12	0.180	23.7	0.31	38
	40.7	19	0.102	38.4	0.23	82
	54.9	53	0.110	48.4	0.24	219
	25.2	8.0	0.140	24.2	0.26	31
Surface Swept (Run 4)	25.2	8.0	0.135	24.2	0.25	32
	40.2	24	0.135	37.3	0.25	95
	55.5	61	0.130	48.0	0.25	243

a. Values for orifice 02 as calculated from data for orifice 01.

b. (Ionization Gauge (IG) reading ÷ Meniscus Area) x 10^7.

TABLE 3

EVAPORATION RATE DATA FOR TIN AMALGAM (52 ppm)

	Wall Temp (°C)	IG[a] Reading x 10^7 (torr)	Meniscus Height, h (cm)	Meniscus Temp, T (°C)	Meniscus Area, A (cm^2)	Relative[b] Evap. Rate per cm^2
Initial Measurements (Run 1)	25.2	11	0.12[c]	23.8	0.25	44
	39.5	29	0.12[c]	35.9	0.25	116
	54.2	56	0.12[c]	47.3	0.25	224
	25.3	7.5	0.135	24.4	0.26	29
Surface Swept (Run 2)	25.7	8.7	0.109	24.6	0.23	38
	39.3	21	0.131	36.7	0.25	84
	55.3	49	0.131	49.2	0.25	196
	25.4	8.1	0.154	24.4	0.28	29
Exposed to Oxygen at 290 N/m^2 for 70 minutes (Run 3)	25.3	0.9	0.135	25.2	0.26	3.5
	40.7	3.7	0.147	40.2	0.27	14
	55.2	11	0.147	53.9	0.27	40
	25.8	0.8	0.120	24.9	0.24	3.3
Surface Swept (Run 4)	25.8	11	0.184	24.4	0.31	35
	40.1	21	0.143	37.5	0.26	81
	54.8	46	0.143	49.1	0.26	177

a. Using orifice 02

b. (Ionization Gauge (IG) reading ÷ Meniscus Area) x 10^7

c. Visual Estimate

TABLE 4

EVAPORATION RATE DATA FOR SODIUM AMALGAM (229 ppm)

	Wall Temp (°C)	IG[a] Reading x 10^7 (torr)	Meniscus Height, h (cm)	Meniscus Temp, T (°C)	Mensicus Area, A. (cm^2)	Relative[b] Evap. Rate per cm^2
Initial Measurements (Run 1)	24.0	12	0.215	22.5	0.35	34
	42.0	29	0.188	38.4	0.32	91
	55.8	37	0.103	51.2	0.23	161
	24.1	3.2	0.035	23.7	0.19	17
Surface Swept (Run 2)	24.1	9.8	0.185	22.9	0.31	32
	40.1	24	0.164	37.1	0.29	84
	53.5	49	0.118	47.4	0.24	205
	22.9	7.5	0.153	22.0	0.27	28
Exposed to Oxygen at 240 N/m^2 for 70 minutes (Run 3)	21.8	0.32	0.298	21.8	0.51	0.63
	41.4	1.0	0.314	41.3	0.55	1.8
	54.5	1.4	0.298	54.3	0.51	2.8
	22.5	0.21	0.181	22.5	0.31	0.68
Surface Swept (Run 4)	21.3	6.9	0.186	20.4	0.31	22
	38.4	20	0.116	35.9	0.24	82
	50.9	44	0.117	45.5	0.24	181
	20.0	6.4	0.150	19.2	0.27	24

a. Using orifice 02

b. (Ionization Gauge (IG) reading ÷ Meniscus Area) x 10^7

TABLE 5

ABSOLUTE EVAPORATION RATES FOR 229 ppm SODIUM AMALGAM
AS DETERMINED VOLUMETRICALLY

Wall Temp. (°C)	Duration of Experiment, t (secs.)	Volume Evaporated, v (μl)	Meniscus Temp., T (°C)	Meniscus Area, A (cm^2)	Evaporation Rate, G ($g \cdot cm^{-2} \cdot sec^{-1}$)	Kinetic Theory Rate for mercury in free space at T°C, Gesc[a] ($g.cm^{-2}\ sec^{-1}$)
20.2	3720	3.0	19.6	0.23	$(4.7 \pm 1.6) \times 10^{-5}$[b]	6.4×10^{-5}
55.0	900	11.2	49.6	0.23	$(7.3 \pm 0.7) \times 10^{-4}$[b]	6.1×10^{-4}

a. calculated from equation (2).

b. indicated errors are those which would result from a 1 μl error in the volume determination.

TABLE 6

EVAPORATION RATE DATA FOR LITHIUM AMALGAM (165 ppm)

	Wall Temp (°C)	IG[a] Reading x 10^7 (torr)	Meniscus Height, h (cm)	Meniscus Temp, T (°C)	Meniscus Area, A cm^2	Relative[b] Evap Rate per cm^2
Initial Measurements (Run 1)	24.7	9.3	0.091	23.5	0.22	42
	40.4	19	0.141	38.0	0.26	75
	55.5	58	0.179	48.3	0.30	193
	24.7	17	0.318	22.7	0.56	30
Surface Swept (Run 2)	24.7	10	0.143	23.4	0.26	40
	41.1	20	0.129	38.7	0.25	79
	54.5	44	0.124	49.1	0.25	174
	25.3	15	0.295	23.5	0.51	29
Exposed to Oxygen at 290 N/m^2 for 70 minutes (Run 3)	25.2	0.96	0.329	25.1	0.59	1.6
	42.2	3.7	0.332	41.7	0.60	6.2
	55.3	4.3	0.235	54.8	0.39	11
	25.4	0.81	0.089	25.3	0.22	3.7
Surface Swept (Run 4)	25.4	6.9	0.128	24.5	0.25	28
	40.7	26	0.208	37.5	0.34	76
	56.2	49	0.183	50.3	0.31	158
	23.8	18	0.328	21.5	0.59	31

a. Using orifice 02

b. (Ionization Gauge (IG) reading ÷ Meniscus Area) x 10^7

TABLE 7

EVAPORATION RATE DATA FOR MERCURY (0.3 ppm Lithium)

Wall Temp (°C)	IG[a] Reading x 10^7 (torr)	Meniscus Height, h (cm)	Meniscus Temp, T (°C)	Meniscus Area, A (cm^2)	Relative[b] Evap Rate per cm^2
24.9	5.5	0.102	24.2	0.23	24
24.9	5.2	0.097	24.3	0.23	23
24.9	6.4	0.150	24.1	0.27	24
40.4	19	0.168	37.5	0.29	65
40.6	18	0.146	37.4	0.27	67
56.8	38	0.050	51.6	0.20	188
56.9	35	0.016	51.9	0.19	186
56.4	67	0.277	48.0	0.47	142
56.4	62	0.256	48.6	0.42	148

a. Using orifice 02

b. (Ionization Gauge (IG) reading ÷ Meniscus Area) x 10^7

TABLE 8

SOURCES OF ERROR IN RELATIVE EVAPORATION RATES

	Source of Error	Estimated Likely Error in Quantity	Estimated Error In Relative Evap. Rate Caused by Est. Error in Quantity	Comments
a.	Non-systematic errors*			
	Ionization Gauge Reading	5%	5%	Includes errors from adjustment of filament current, reading of meter, etc.
	Wall Temp.	0.3°C	3%	Temp is average of four thermocouple readings.
	Meniscus Height	0.005 cm	2%	Errors in height lead to errors in area; area is calculated assuming elliptical cross-section. The error would be greater where the cross-section was circular.
	Meniscus Temp.	0.5°C	4%	Reflect errors in ionization gauge readings.
b.	Systematic errors			
	Orifice Conductivity Ratio (02/01)	5%	5%	The most likely error, an underestimate of the diameter of 01, would cause the rates for the first experiment (pure mercury) to be too high.
	Ionization Gauge Sensitivity	40%	40%	The first and last sets of data for mercury indicate a change in sensitivity of this magnitude.
	Meniscus Temp. Correction	0.5°C	4%	Errors from these sources should tend to cancel out in relative measurements.
	Meniscus Area	5%	5%	

* Average SEE of log (evap. rate) = 0.074; this represents a standard error of 18% in the evaporation rate whereas only about 8% can be accounted for by the estimates of the non-systematic errors.

TABLE 9

REGRESSION EQUATIONS RELATING RELATIVE EVAPORATION RATE PER UNIT AREA TO ABSOLUTE TEMPERATURE

System	Constants in Regression Equation[a]		Standard Error of Estimate
	Intercept	Regression Coefficient	
Clean Surfaces			
Pure mercury	12.13	$(-3.14 \pm 0.18) \times 10^3$	0.073
Pure mercury (0.3 ppm Li)	11.71	$(-3.07 \pm 0.06) \times 10^3$	0.022
Tim amalgam (52 ppm)	11.56	$(-2.98 \pm 0.25) \times 10^3$	0.088
Sodium amalgam (229 ppm)	11.58	$(-3.00 \pm 0.25) \times 10^3$	0.106
Lithium amalgam (165 ppm)	10.27	$(-2.60 \pm 0.17) \times 10^3$	0.069
Following Exposure to Oxygen			
Tin amalgam (52 ppm)	12.97	$(-3.71 \pm 0.08) \times 10^3$	0.019
Sodium amalgam (229 ppm)	6.47	$(-1.96 \pm 0.10) \times 10^3$	0.028
Lithium amalgam (165 ppm)	7.80	$(-2.21 \pm 0.73) \times 10^3$	0.183

a. $\log_{10}$ (evaporation rate per unit area) = intercept + (regression coeff.)/T°K

TABLE 10

CALIBRATION OF IONIZATION GAUGE AND ORIFICE 02 FOR PRESSURE MEASUREMENTS USING THE SATURATED VAPOR PRESSURES OF MERCURY

Temp (°C)	Gauge Reading, P_{ig} (torr)	Vapor Pressure, P_{sat} (torr)	P_{sat}/P_{ig}
23.0	2.90×10^{-5}	1.76×10^{-3}	61
23.0	1.45×10^{-5}	1.76×10^{-3}	121
22.8	1.40×10^{-5}	1.73×10^{-3}	124
24.9	2.03×10^{-5}	2.06×10^{-3}[a]	101
		Average value of calibration factor	102

a. This data is for the lithium amalgam.

TABLE 11

CALCULATED RATES OF EVAPORATION OF MERCURY AND AMALGAMS IN FREE SPACE

	Rate of Evaporation x 10^4 ($g.cm^{-2}.sec^{-1}$)		
	25°	40°	55°
Pure Mercury and the amalgams	1.0 ± 0.15	3.0 ± 0.45	8.5 ± 1.3
O_2-treated tin amalgam (52 ppm Sn)	0.095	0.32	1.3
O_2-treated sodium amalgam (229 ppm Na)	0.025	0.048	0.088
O_2-treated lithium amalgam (165 ppm Li)	0.085	0.19	0.32

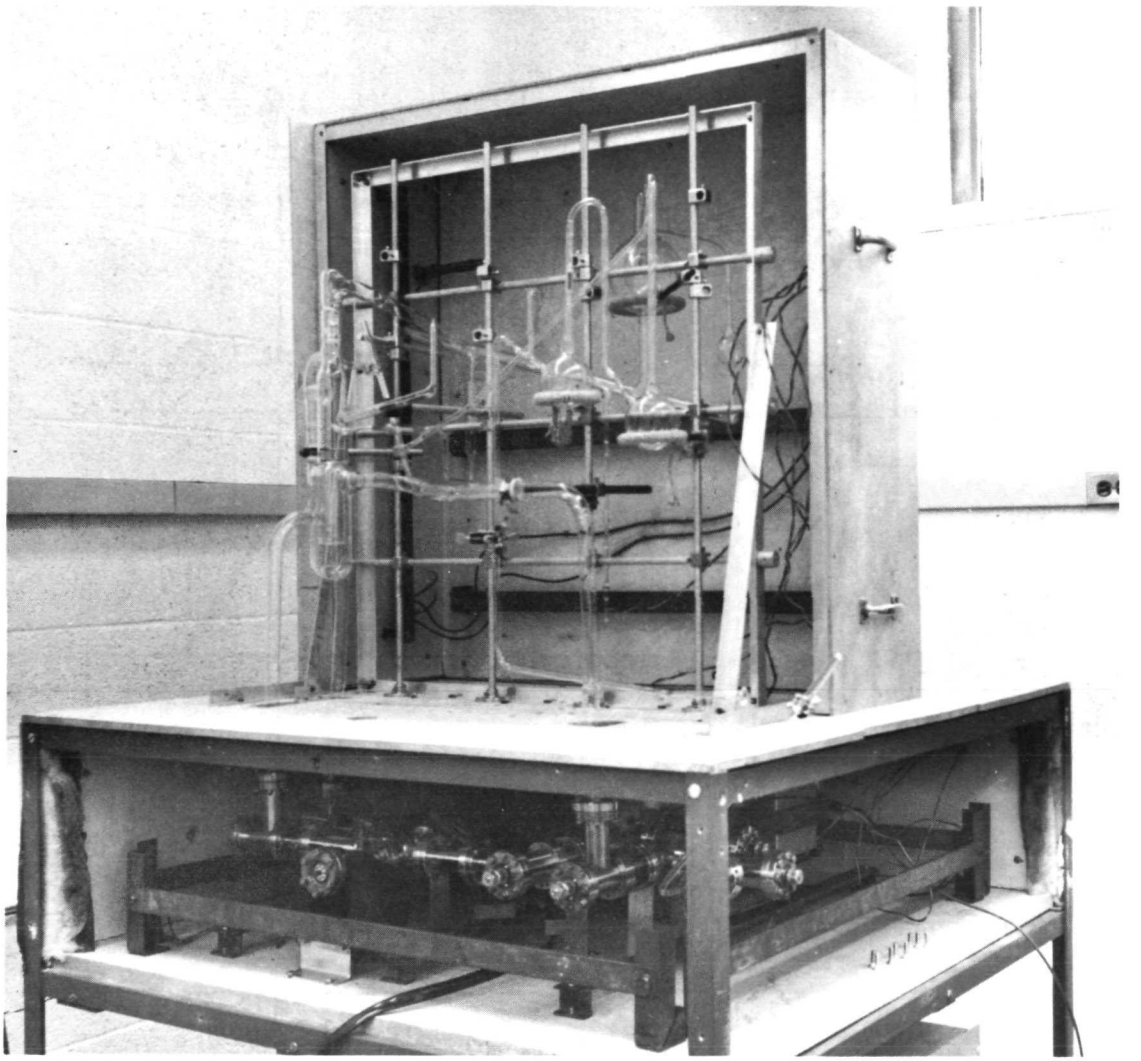

Figure 1. Photograph of Apparatus at Start of First Experiment with Pure Mercury.
(Half of the upper furnace is in place ready for bake-out and two of the side panels are in place on the lower furnace.)

Figure 2. Pumping and Pressure Measuring System.

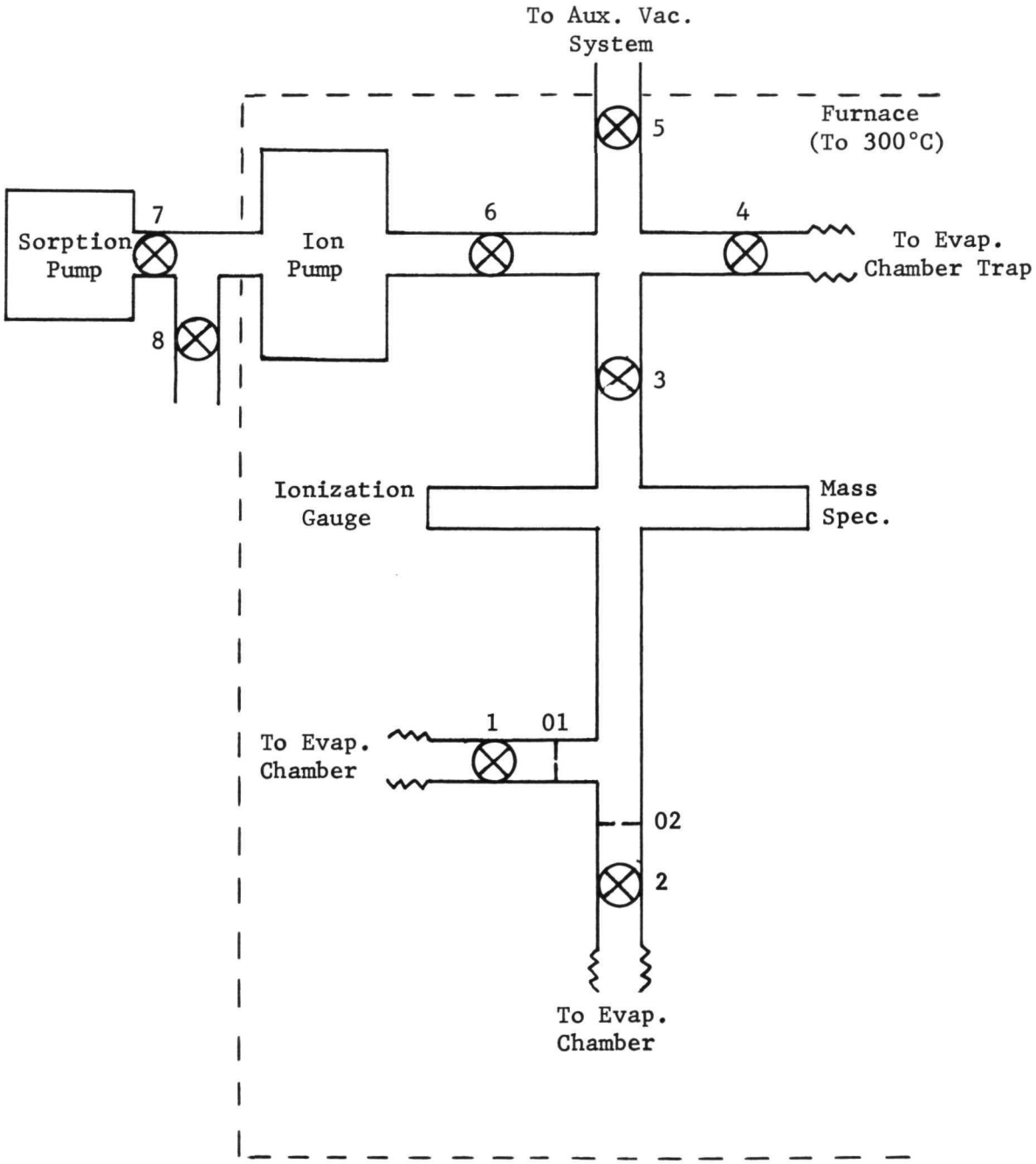

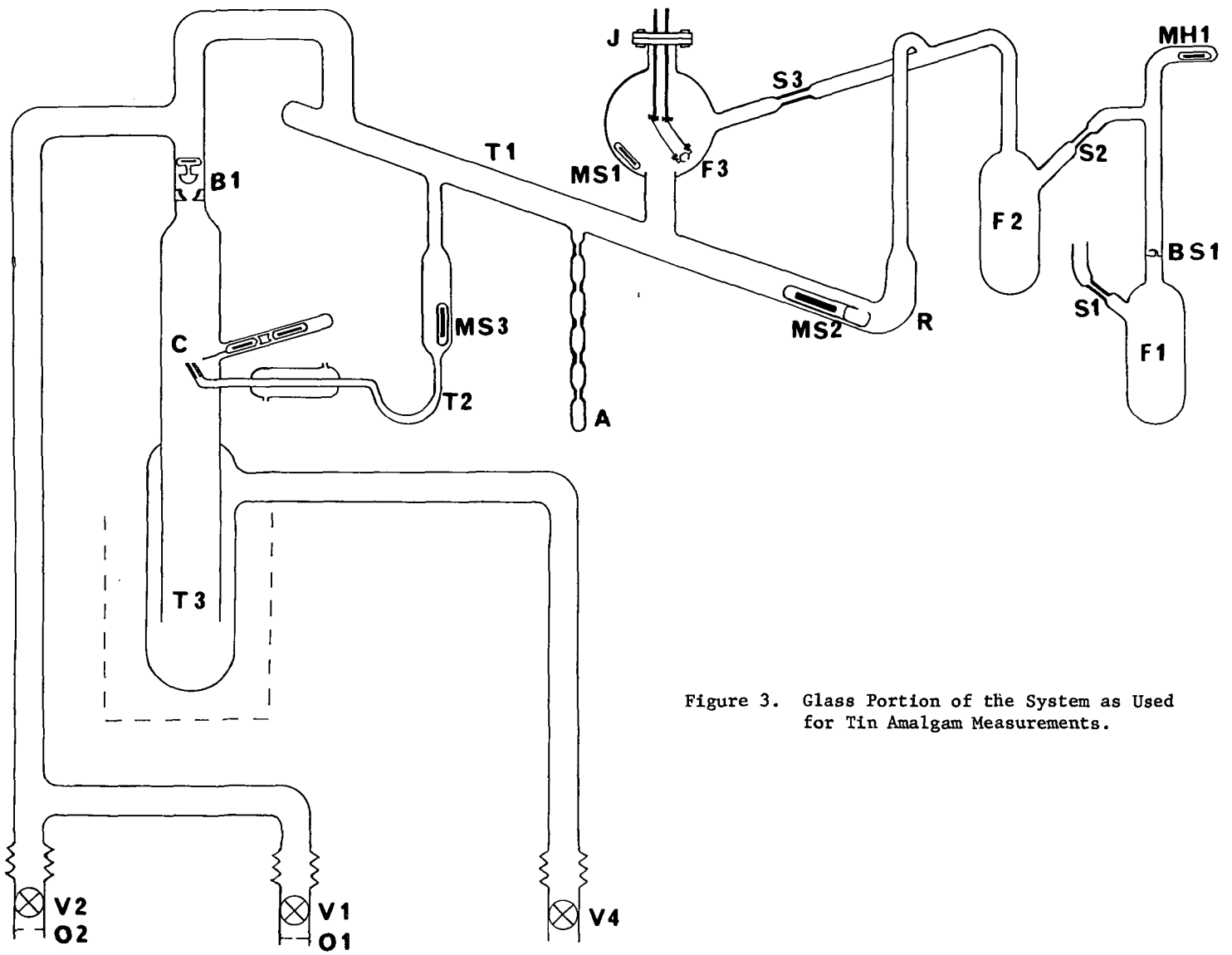

Figure 3. Glass Portion of the System as Used for Tin Amalgam Measurements.

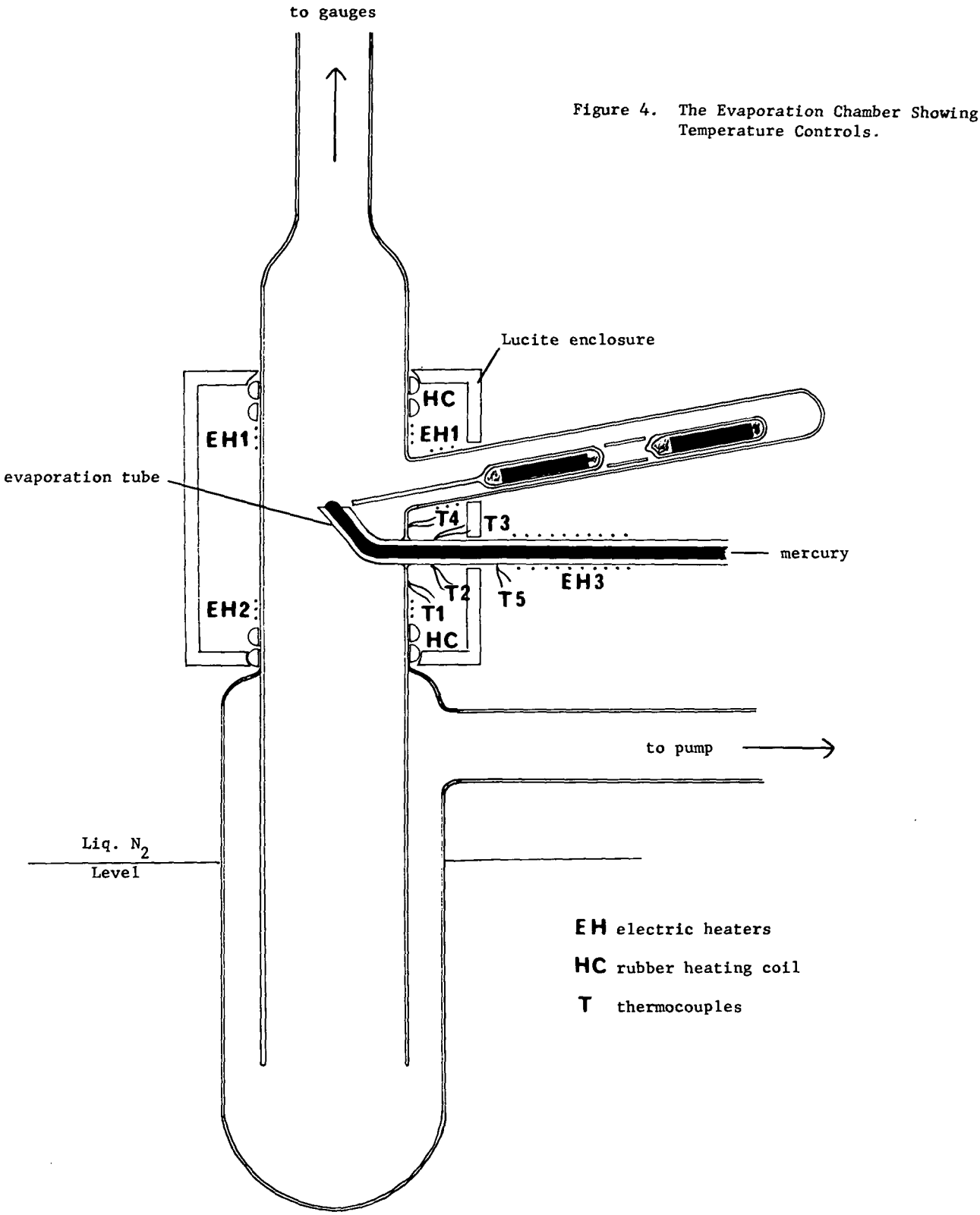

Figure 4. The Evaporation Chamber Showing Temperature Controls.

Figure 5. Evaporation Rates for Pure Mercury.

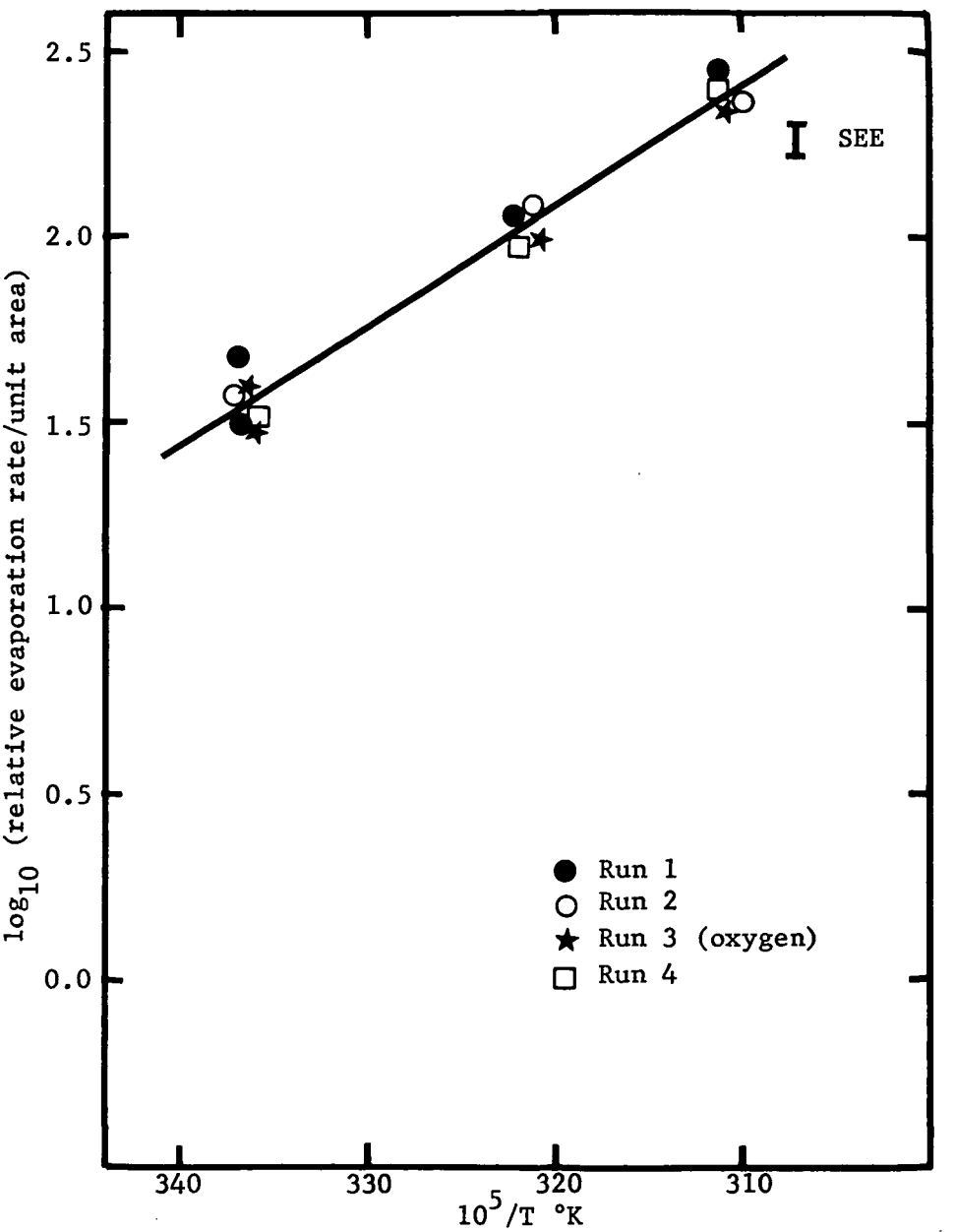

Figure 6. Evaporation Rates for Tin Amalgam.

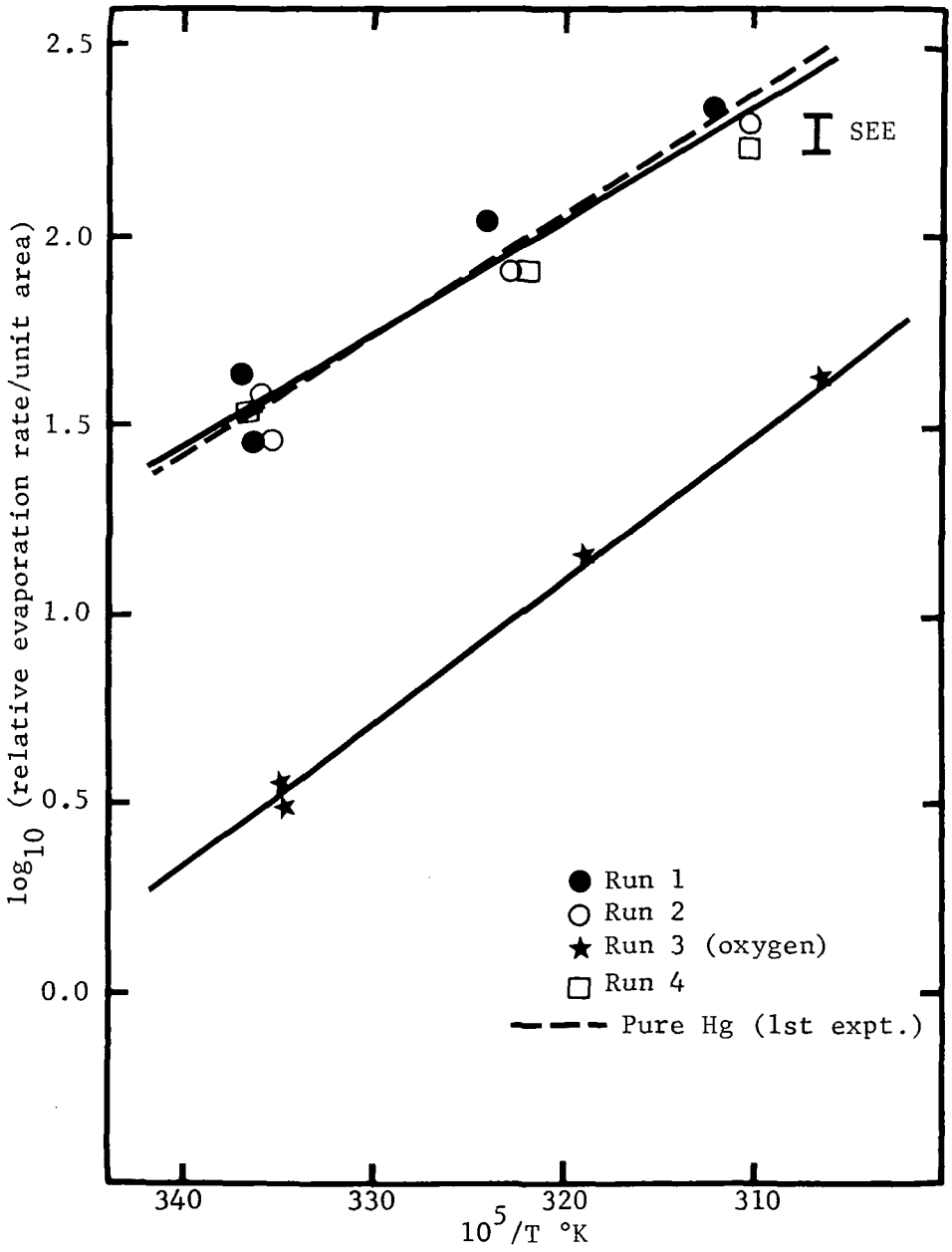

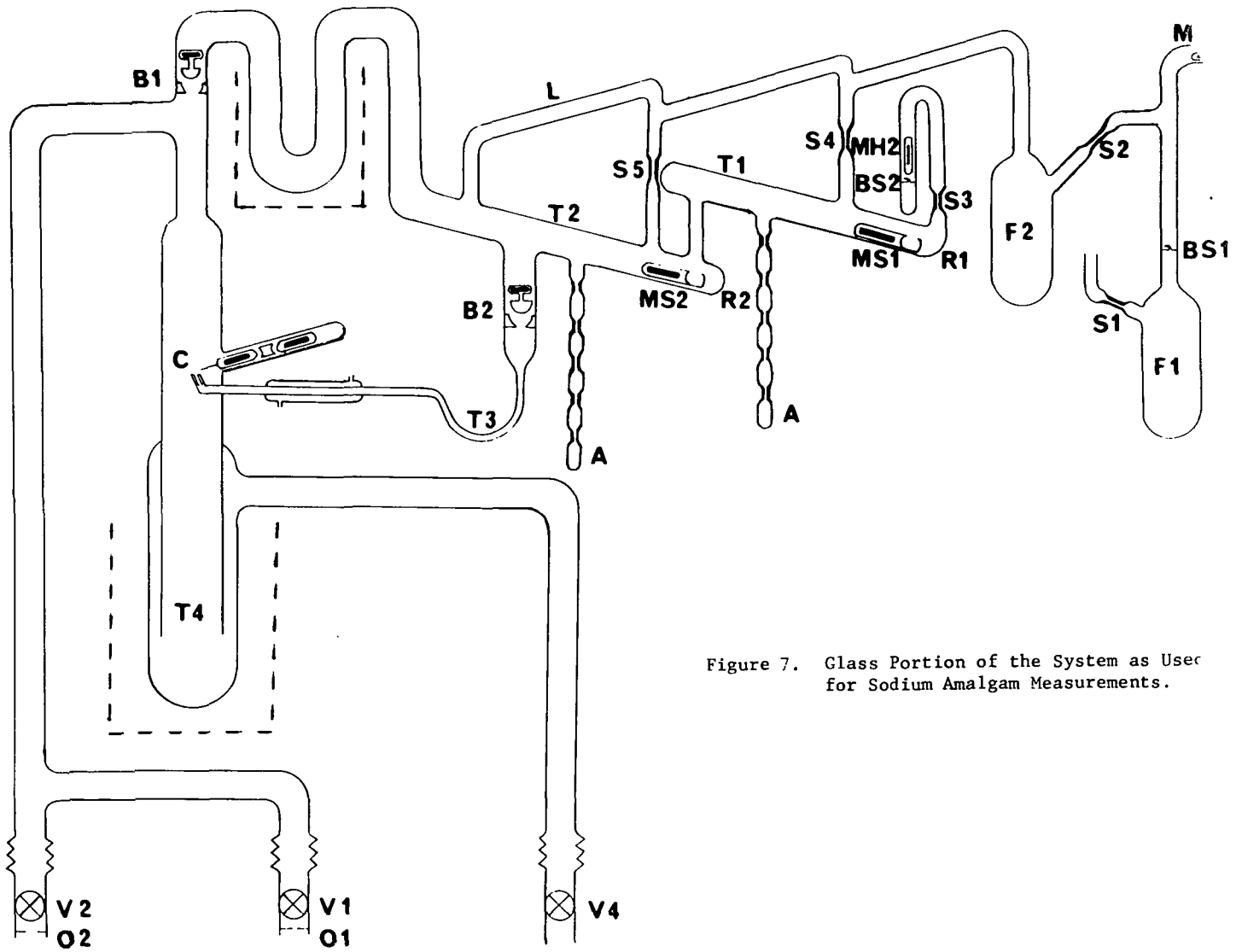

Figure 7. Glass Portion of the System as Used for Sodium Amalgam Measurements.

Figure 8. Evaporation Rates for Sodium Amalgam.

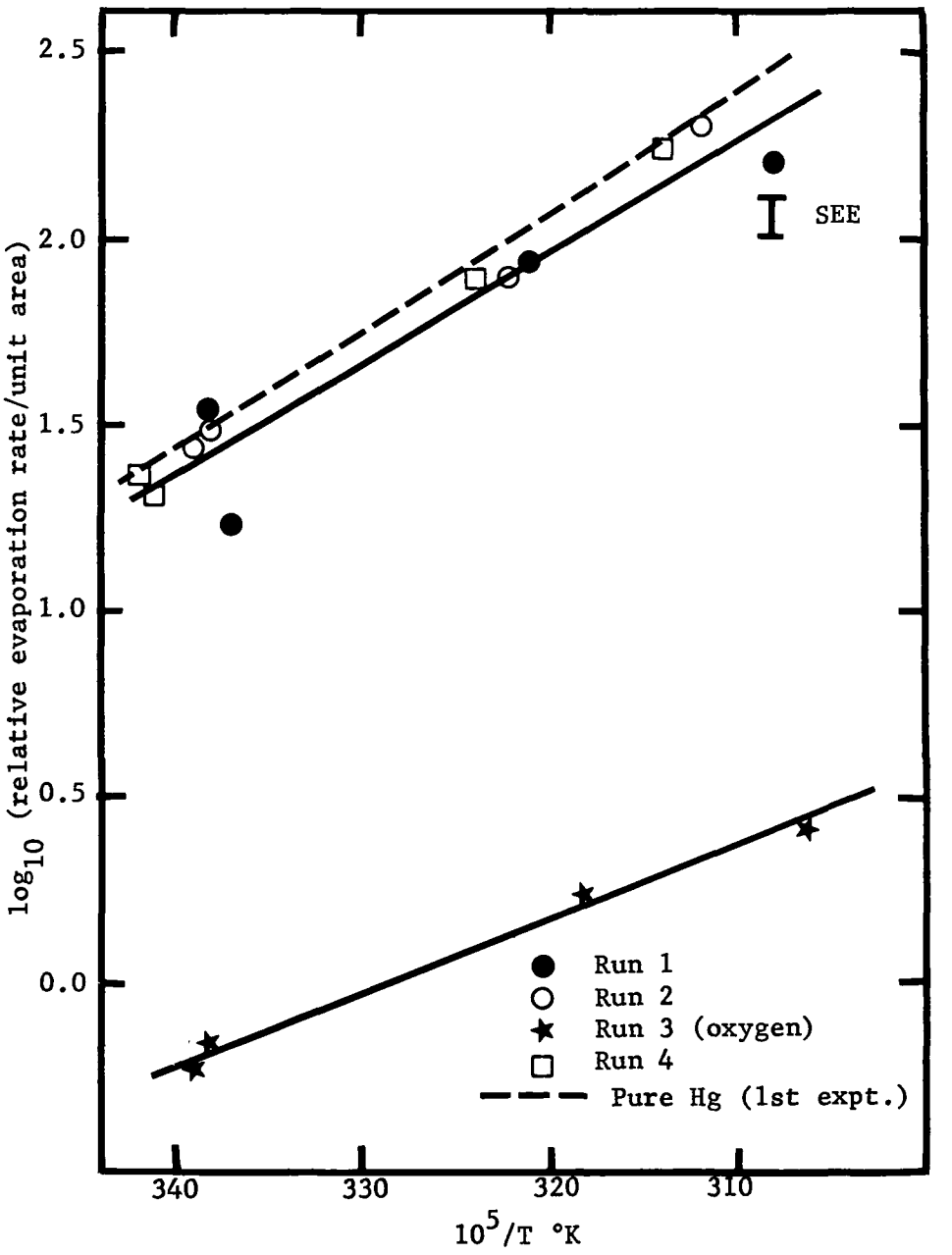

Figure 9. Ionization Gauge Chart Recording During Break Away of Lithium Amalgam Drop.

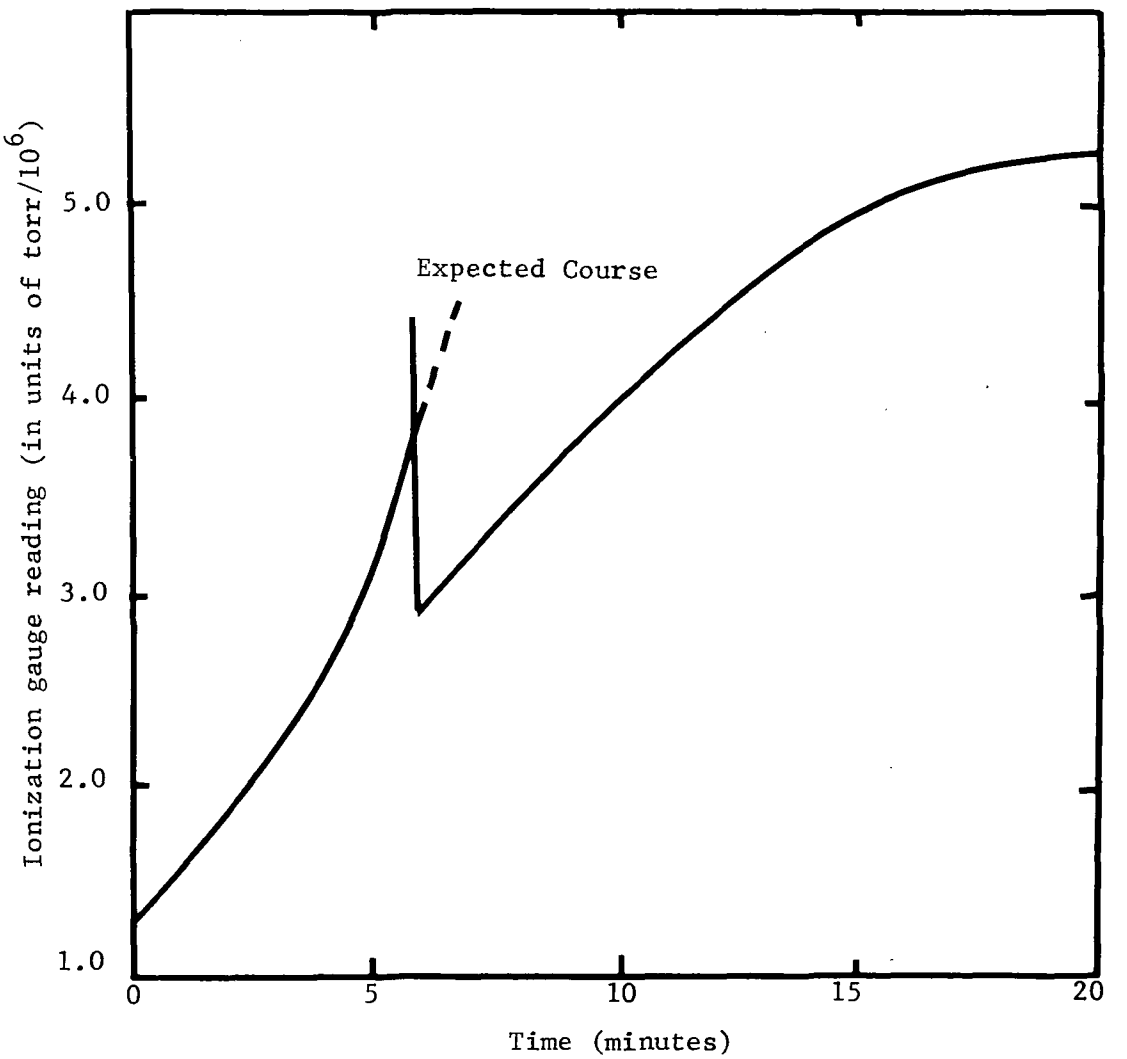

While heating the amalgam from 40° to 55°C in Run 3, a portion of the meniscus broke away and fell into the trap. The instantaneous increase in pressure followed by a pressure decrease is attributed to a reduction in area and healing of the surface film.

Figure 10. Evaporation Rates for Lithium Amalgam.

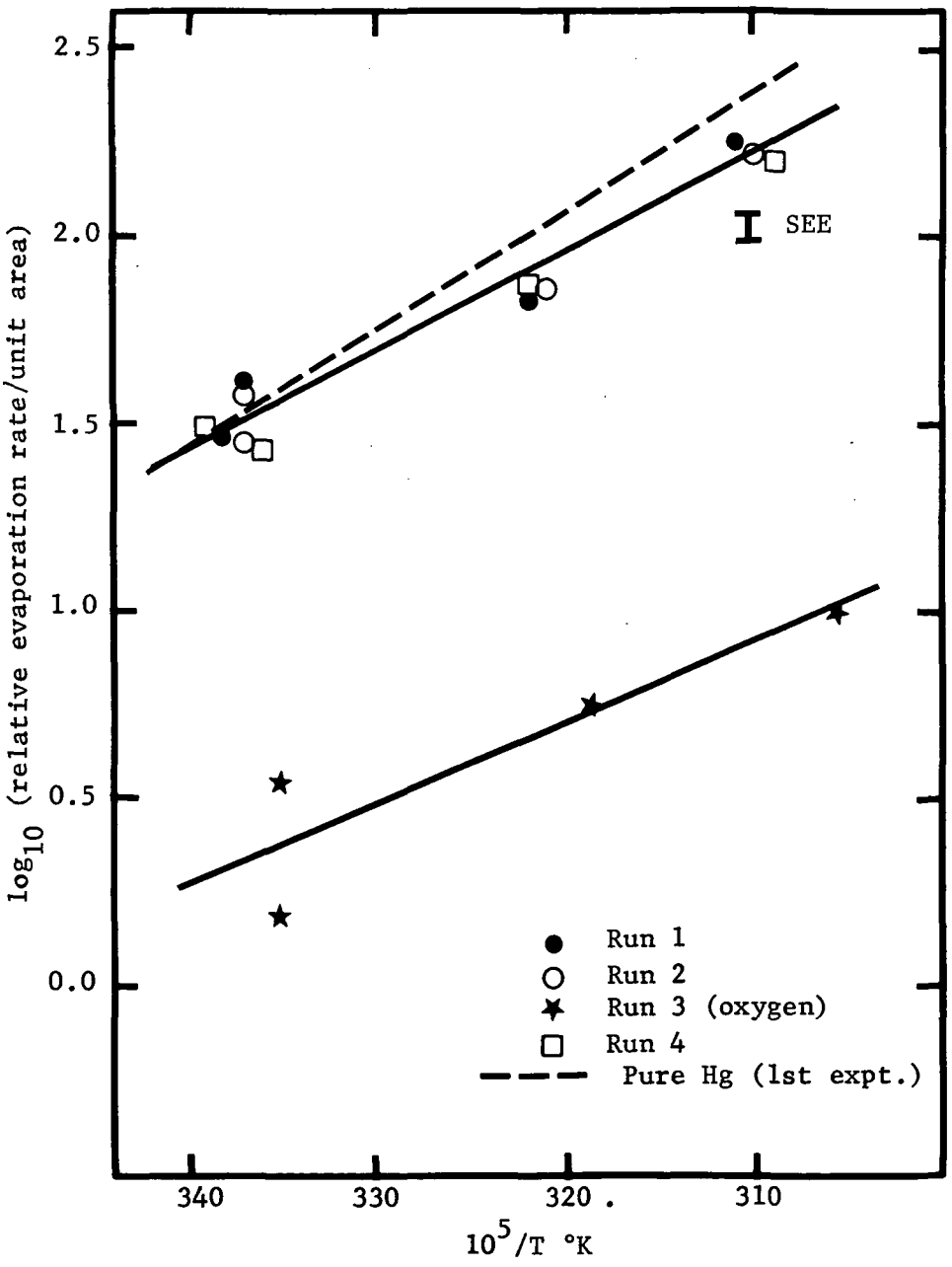

Figure 11. Evaporation Rates for Pure Mercury (0.3 ppm Li).

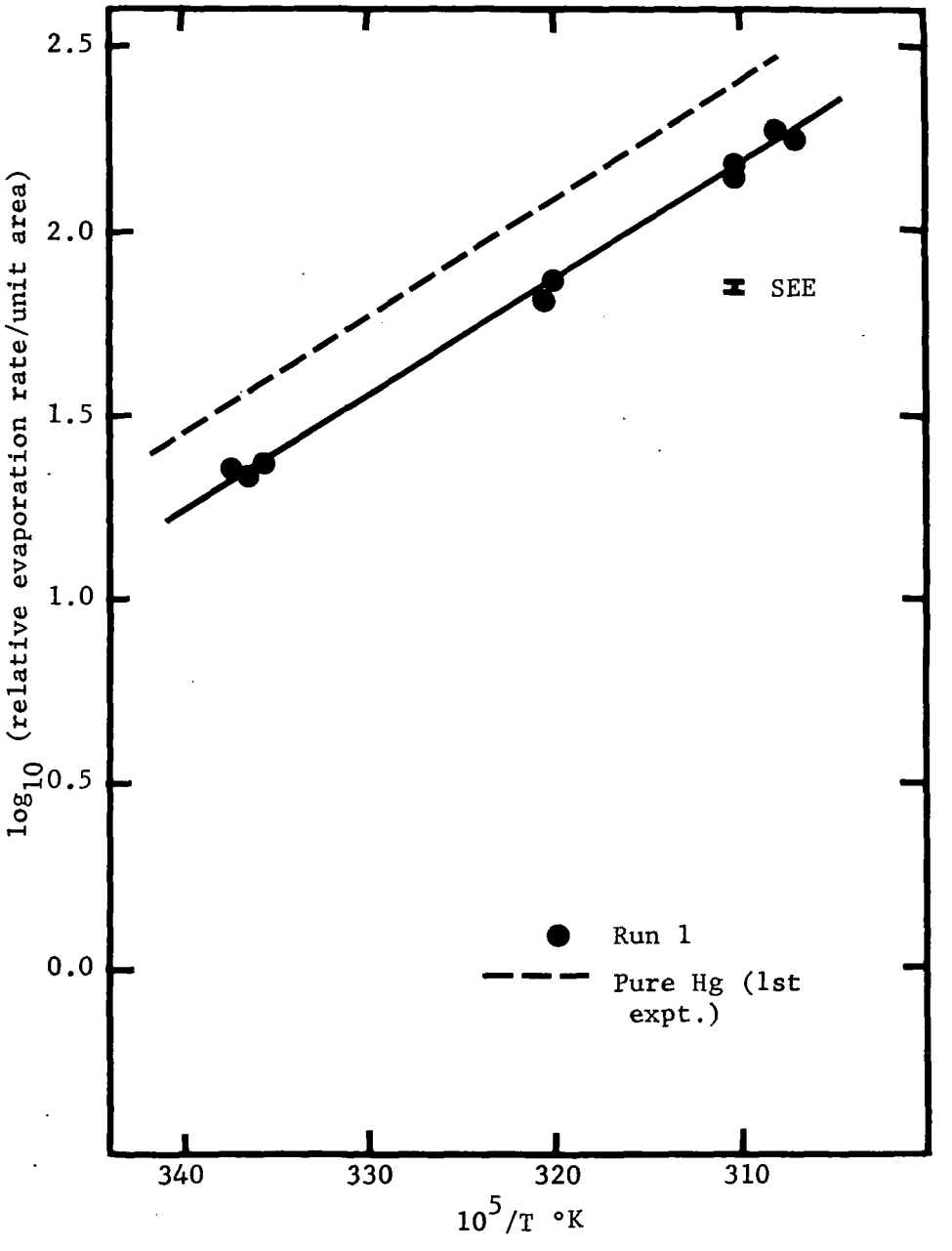

Figure 12. Evaporation Rates for Mercury and Amalgams.

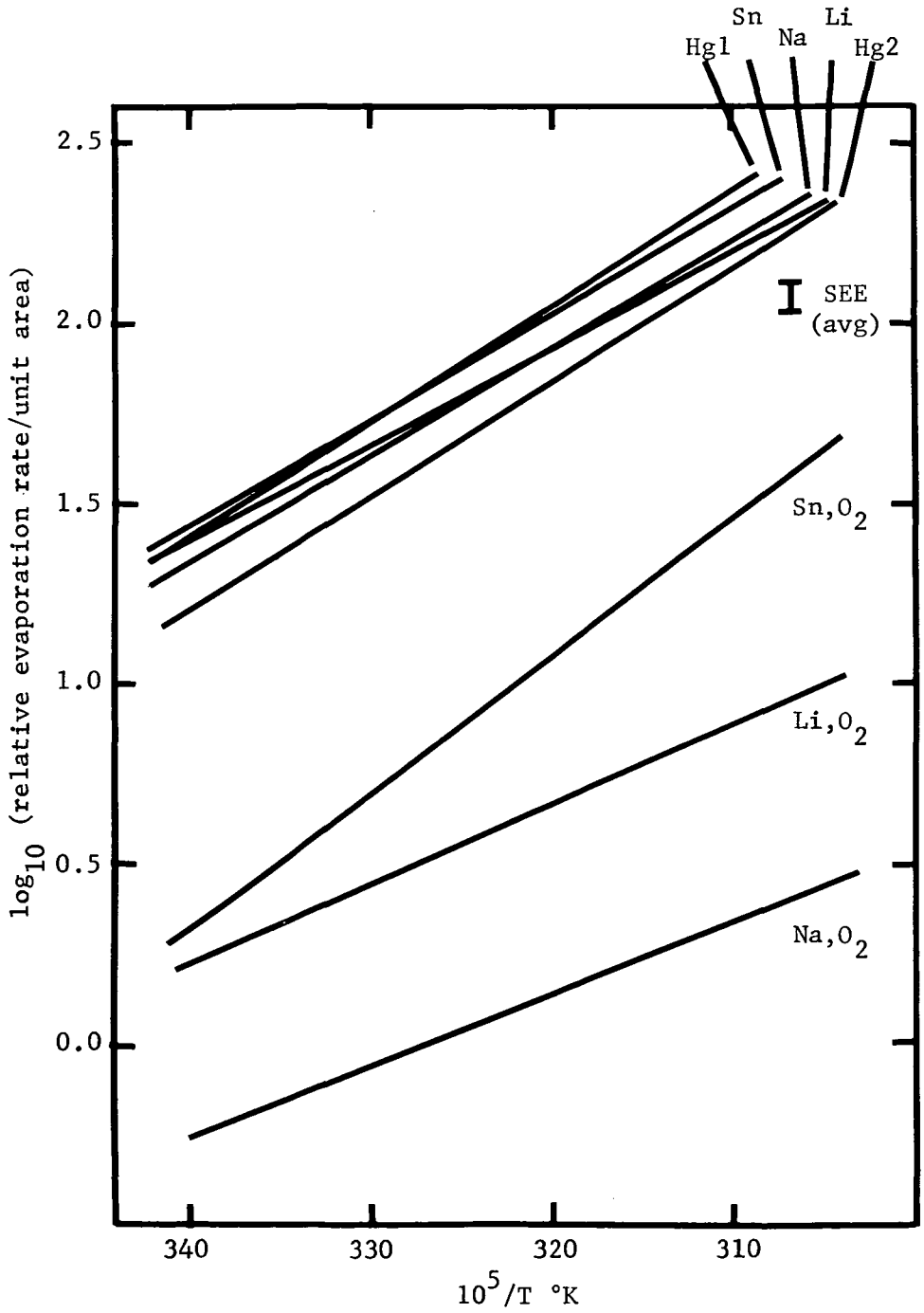

Figure 13. Evaporation Rate Regression Lines (Corrected for Changes in Gauge Sensitivity).

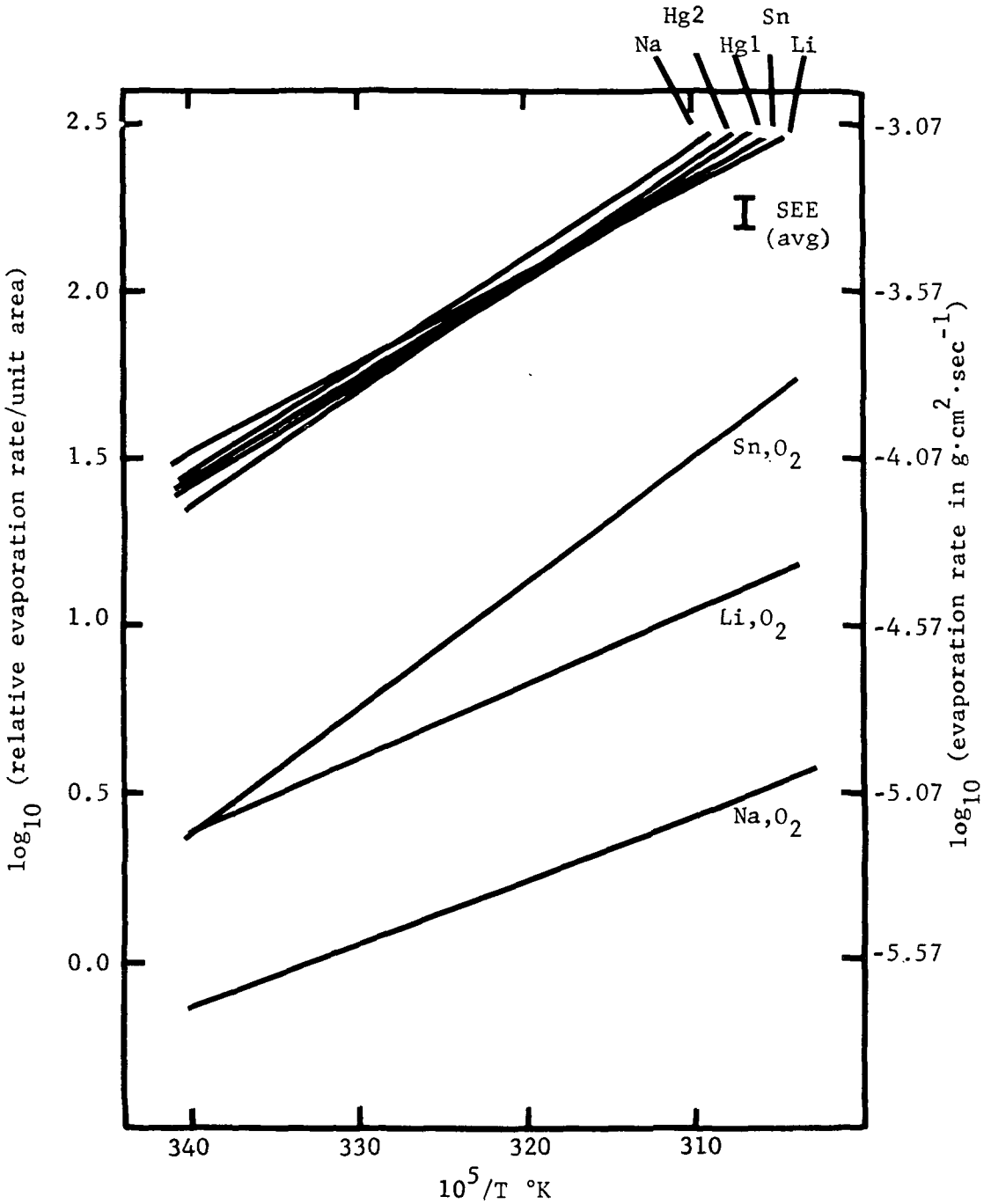

APPENDIX I

SURFACE EXCESS CONCENTRATIONS OF ALKALI METALS IN AMALGAMS

The surface excess concentration $\Gamma 2$ of a solute at the solvent interface can be calculated if the relationship between solute concentration C_2 and surface tension γ is known. The calculation makes use of the Gibbs equation

$$\Gamma_2 = -\frac{C_2}{RT} \cdot \frac{\partial \gamma}{\partial C_2}$$

in which R is the gas constant and T is the absolute temperature.

In the case of amalgams, the most comprehensive compilation of surface tension data is that given by Semenchenko (12). The data presented suggest that the surface tensions of some 0.001 mole fraction amalgams are (in dynes. cm^{-1}) Sn, 400; Li, 360; Na, 340; K, 280; Rb, 240; Cs, 230. Thus, in the alkali metal series, the surface activity increases with atomic weight, with cesium being very much more surface active than lithium or sodium.

To indicate the surface excess concentration of a 200 ppm solution of sodium in mercury, the surface tension data of Semenchenko for 25°C may be used:

Na concn., C_2 (moles/l)	C_2 (ppm)	γ (dynes/cm)	γ, calc. (dynes/cm)
0.00305	5.1	386	382
0.00537	9.1	368	366
0.0167	28	354	346
0.0523	88	328	338
0.0911	154	337	336

The data in the third column can, to a sufficiently good approximation, be fitted by the hyperbola:

$$\gamma = \frac{0.22}{C_2 + 0.0015} + 334$$

where C_2 is in moles/l. Values of γ calculated using this expression are tabulated in the right hand column of the table to indicate the goodness of fit. By differention of this expression for γ with respect to C_2, and then substituting the value of $C_2 = 0.118$ mole/l, it may be calculated that $d\gamma/dC_2 = -15.2$ dynes. cm^{-1} $mole^{-1}$. liter for a 200 ppm sodium amalgam. Using the known values of C_2, $d\gamma/dC_2$, R and T in the Gibbs equation, it may be calculated that:

$$\Gamma_2 = 7.3 \times 10^{-11} \text{ moles.cm}^{-2}$$

$$= 4.38 \times 10^{-3} \text{ molecules.} \overset{\circ}{A}^{-2}$$

This implies that the area occupied per excess sodium atom in the surface is 230 A^2. If the effective area of a sodium atom is 10 A^2 and if the surface excess is localized in the outermost layer of atoms, then sodium atoms will occupy about 5% of the total surface area of a 200 ppm sodium amalgam.

APPENDIX II

MATERIALS

A. Pure Mercury

The mercury used was triple distilled instrument mercury obtained from the Bethlehem Apparatus Company*. The supplier's Certificate of Analysis stated that the total residue on evaporation did not exceed one part in ten million.

B. Pure Tin

The tin was obtained from the Ventron Company in the form of 0.025 cm (10 mil) wire. The supplier stated the purity to be 99.999% in terms of metal content. Inevitably, some contamination, particularly by oxidation, must have occurred during the wire-forming process.

C. Pure Lithium

The lithium was obtained from the Ventron Company in the form of a 5.08 cm (2 in) wide, 0.038 cm (15 mil) thick ribbon packed in argon. The stated purity of the lithium was 99.95% in terms of the metal content, but its dull appearance indicated a quite thick layer of corrosion product, presumably oxide or nitride.

D. Pure Sodium

The sodium was obtained from the Ventron Company in a glass ampoule sealed off under argon. The stated purity of the sodium was 99.95% in terms of total impurities. Typical impurity levels of sodium in this form are (in ppm) K, 40; C, 20; Si, 20; O, 10; Rb, 10; others, less than 5.

E. Pure Oxygen

The oxygen was obtained from the Airco Company in a 1 liter borosilicate glass flask with a break seal. The purity of the oxygen was stated to be 99.995%.

F. Standard Solutions

The 1000 ppm standard solutions of tin, sodium and lithium used in analyses of extracts from the amalgams were obtained from the Aztec Instrument Company.

---

*Supplier's names are given for completeness of description. Their use is not intended to imply special endorsement of the products.

APPENDIX III

CALCULATION OF THE MENISCUS SURFACE AREA AND VOLUME FROM THE MENISCUS HEIGHT

Meniscus Surface Areas

The opening in the precision bore evaporation tube was elliptical since the tube was cut off and ground at 45° to its axis (see Figure 4). Measurements of the major and minor axes of the ellipse showed them to be 0.488 and 0.410 cm, respectively. Except in rare cases, the meniscus was adjusted so that its base exactly coincided with the elliptical opening in the tube. However, due to the evaporation, the meniscus height could not be held constant. It was therefore necessary to find a way of determining the meniscus area so that changes in area could be taken into account when intercomparing evaporation rates.

Since the base of the meniscus was usually fixed by the tube opening (as in Figure 14(a)), it appeared that the meniscus area should be a function only of the meniscus height. It was then assumed that the meniscus could be approximated by the unique prolate spheroid sitting on the elliptical tube opening which projected to the meniscus height h above the plane of the opening. However, to simplify the calculations of the areas of segments of the prolate spheroids above the opening, it was further assumed that the areas of the spheroids were simply related to the areas of the spheres of the same heights sitting on a circular base of the same area as the elliptical opening. The exact comparisons between the properties of the spheroids and the corresponding spheres are summarized in Figure 14. Many of the expressions listed are well known, e.g., see ref (24), and the others are easily derived from the standard ones.

Using the known dimensions of the axes of the ellipse and expressions from (6) of Figure 14, it was shown that, when the portion of the spheroid above the plane xx of the opening was a hemispheroid, its surface area was 13% larger than the area of the spherical segment of the same height on a base of the same area. Also, since, for h = 0, the spheroidal and spherical surfaces had the same area, it appeared that a reasonable approximation to the area of the spheroidal segment, height h, up to the height of the hemispheroid, would be the area of the spherical segment plus a correction which increased linearly from 0 to 13% of its area as h increased from 0 to 0.205 cm, the height of the hemispheroid. A similar calculation was made for heights greater than that of the hemispheroid. Here, the area of the meniscus was calculated as the difference between the total area of the complete spheroid defined by the elliptical base and height h, and the area of the portion of the spheroid below the base; the area of the portion below the base was approximated by comparison with the area of a portion of a sphere in exactly the same way as described for the smaller menisci. The derived curve which was used in the work described in this report is shown as Figure 15. The meniscus heights were measured to ± 0.002 cm using a cathetometer.

Figure 14. Relationships between Areas and Volumes of Prolate Spheroids and Spheres Sitting on a Defined Ellipse or a Circle of Equal Area.

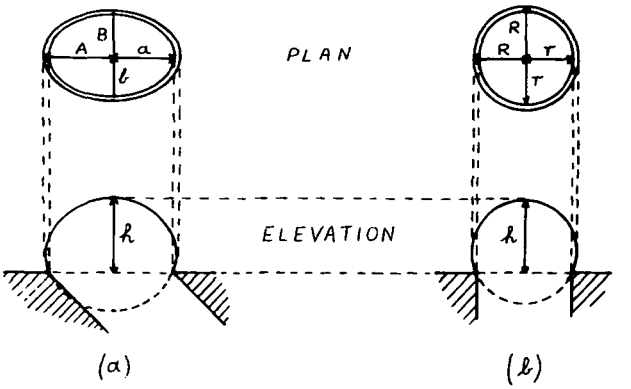

	Prolate Spheroid Sitting on Ellipse (Semi-axes: a,b)	Sphere Sitting on Circle (radius r, where $r^2 = ab$)
1.	Semi-axes of spheroid: A (major), B (minor)	Radius of sphere: R
2.	Area of ellipse: πab	Area of circle: πab
3.	Height above xx: h	Height above xx: h
4.	Expressions for A and B: $A = \frac{a}{b}\left(\frac{b^2+h^2}{2h}\right)$ $B = \left(\frac{b^2+h^2}{2h}\right)$	Expressions for R: $R = \left(\frac{r^2+h^2}{2h}\right)$ $= \left(\frac{ab+h^2}{2h}\right)$
5.	Area of complete spheroid: $2\pi\left(\frac{b^2+h^2}{2h}\right)^2\left(1+\frac{a}{b}\cdot\frac{\sin^{-1}\epsilon}{\epsilon}\right)$ $\epsilon^2 = \left(1-\frac{b^2}{a^2}\right)$	Area of complete sphere: $\pi\left(\frac{r^2+h^2}{h}\right)^2 = \pi\left(\frac{ab+h^2}{h}\right)^2$
6.	(a) Height of hemispheroid sitting on ellipse: b	(a) Area of segment of sphere of height h above xx: $\pi\left(r^2+h^2\right) = \pi\left(ab+h^2\right)$
	(b) Area of hemispheroid: $2\pi b^2\left(1+\frac{a}{b}\cdot\frac{\sin^{-1}\epsilon}{\epsilon}\right)$	(b) Area of segment of sphere of height b above xx: $\pi(ab+b^2)$
7.	Volume of complete spheroid: $\frac{4}{3}\pi\frac{a}{b}\left(\frac{b^2+h^2}{2h}\right)^3$	Volume of complete sphere: $\frac{4}{3}\pi\left(\frac{ab+h^2}{2h}\right)^3$
8.	Volume of hemispheroid, height b, sitting on ellipse: $\frac{2}{3}\pi ab^2$	Volume of segment of sphere, height b, sitting on circle: $\frac{1}{6}\pi b^2\left(b+3a\right)$

As an experimental check on the correctness of the surface area calculation, relative evaporation rates for mercury were measured over a range of meniscus heights corresponding to areas between 0.19 and 0.25 cm^2. It was found that, after applying the necessary temperature correction as described in Appendix IV, the quantity (relative evaporation rate/area x P_{sat}) was a constant, as it should be, to within about 2%. This test provided evidence that the combined area and temperature corrections were of the correct order of magnitude. A similar demonstration of the consistency of the corrections is given by entries in the last four rows of Table 7. Although the meniscus areas differed by as much as 0.27 cm^2 and the meniscus temperatures differed by as much as 3.9°C, the four corrected values all lie close to the regression line of Figure 11 at its upper end.

Meniscus Volume

As mentioned above, the meniscus areas were calculated as the areas of a portion of a prolate spheroid using the convenient approximation based on the area of the section of a sphere of the same base area and same height. A similar approach was taken to the calculation of meniscus volumes. In this case, the correction needed to deduce the volume of the hemispheroid from the volume of the spherical segment of the same base area and same height was only about 6%. Once again, the correction was assumed to vary linearly from 0 to 6% as h varied from 0 to 0.205 cm. The curve relating meniscus volume to meniscus height is shown as Figure 16. It was used in calculating the change in volume of the meniscus during the volumetric measurements of the rate of evaporation of the sodium amalgam.

Figure 15. Relationship Between Meniscus Height and Area.

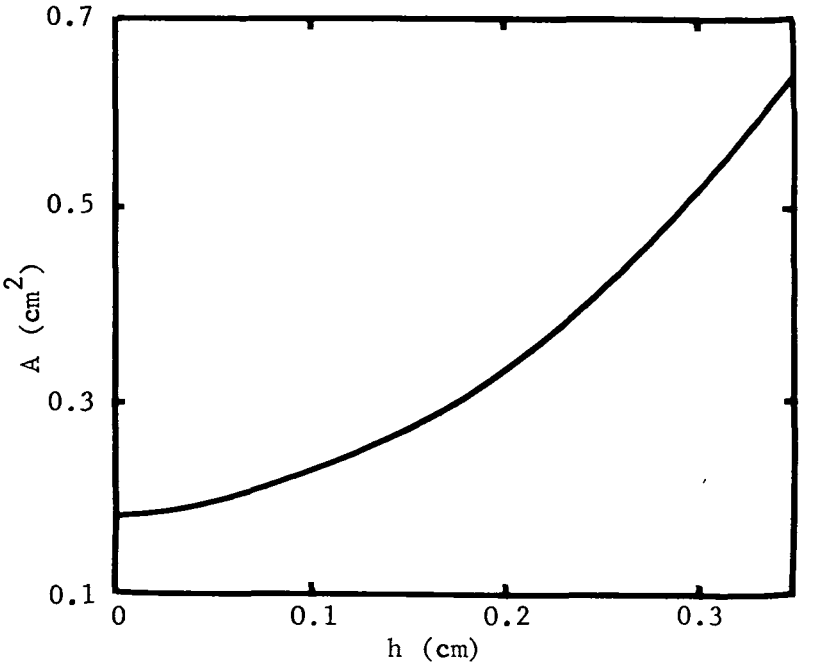

Figure 16. Relationship Between Meniscus Height and Volume.

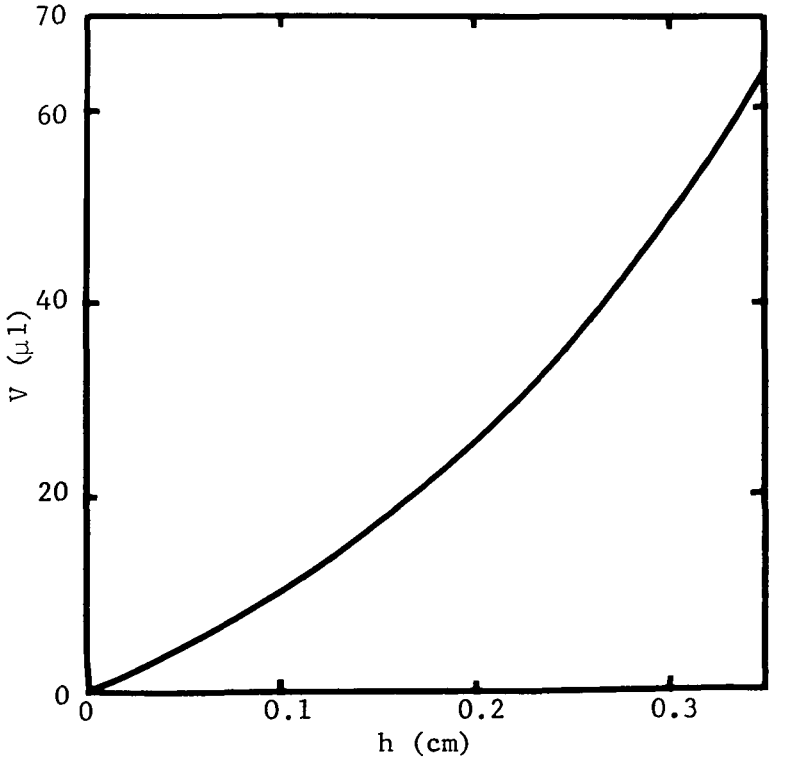

APPENDIX IV

TEMPERATURE CORRECTIONS FOR THE EVAPORATIVE COOLING OF THE MENISCUS

The evaporation tube and meniscus were as sketched in Figure 17. Although the temperature T_w of the wall at the point of entry of the evaporation tube was fixed for each set of measurements, the temperature T at the evaporation surface was always lower due to evaporative cooling. Since T could not be measured directly, it was calculated from T_w by application of a correction ΔT. Clearly, ΔT was directly proportional to the rate of evaporation and, hence, to the ionization gauge readings of Tables 2, 3, 4, 6, and 7.

To find the factor relating gauge reading to ΔT, the data in Table 7 were used. The method was to calculate the temperature differences which must have existed between the evaporation surfaces when T_w was nominally 25°, 40° and 55° if the relative evaporation rate was proportional to P_{sat}, the saturation vapor pressure. It was then calculated that ΔT could be expressed by:

$$\Delta T = \text{Ionization Gauge Reading (torr)} \times (-0.124 \times 10^{7})\,^{\circ}C.$$

This relationship was used to correct all the data in this report.

As a check on the correctness of the expression for ΔT, the thermal conductivity of the evaporation tube from meniscus to wall was calculated. The calculations were for a 2.6 cm long, straight borosilicate glass tube (0.408 cm. i.d., 0.808 cm o.d.) filled with mercury, the length being the estimated length of the axis of the actual, bent evaporation tube. The specific thermal conductivities of the borosilicate glass and mercury were taken to be 11.7×10^{-3} joule·cm^{-1}·sec^{-1}·deg^{-1} and 92×10^{-3} joule·cm^{-1}·sec^{-1}·deg^{-1}, respectively (3,23). The thermal conductivity of the filled tube was then calculated to be 63×10^{-4} joule·sec^{-1}·deg^{-1}. Next, the rate of evaporation from a 0.25 cm meniscus at 50°C was calculated from equation (2); it was 1.7×10^{-4} g.sec^{-1}. Since the heat of vaporization of mercury at 50°C is 302 joule·g^{-1}, the heat loss from this meniscus at 50°C could be calculated to be 5.15×10^{-2} joule·sec^{-1}. The temperature difference, ΔT, necessary to maintain this rate of heat flow along the path of the calculated conductance was 8.2°C. This was in general accord with, but about 15% higher than, the values of about 7°C determined by the method previously described. In view of the inaccuracies in the measurements of the tube geometry, this degree of agreement is satisfactory.

Figure 17. Evaporation Tube Dimensions and Position in Evaporation Chamber.

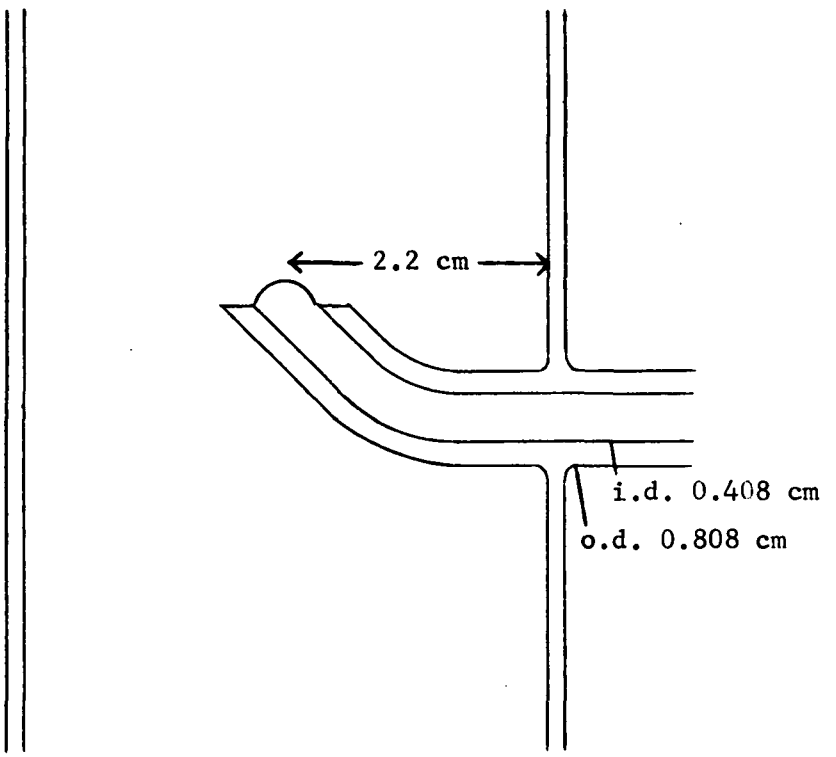

APPENDIX V

ANALYSIS OF AMALGAMS

The concentrations of the amalgams were determined by atomic absorption spectrophotometry of acid extracts. Since the most suitable concentration ranges for accurate analysis were tin, 0-200 ppm; sodium, 0-3 ppm; and lithium, 0-10 ppm, standard solutions in these ranges were prepared by distilled water dilution of 1000 ppm standard solutions (see Appendix II). All the analyses are believed to be correct to within ± 1% of the quantity present.

Tin Amalgam

For tin analysis, a weighed quantity of amalgam was mechanically shaken with 2 ml of concentrated HCl for 5 minutes. Then the acid extract and further distilled water washings of the amalgam were combined and diluted to the 0-200 ppm concentration range. Readings of the spectrophotometer were taken for the extract and for the standard solutions. From the results, the weight of tin in the original weighed quantity of amalgam was calculated. The completeness of the extraction was confirmed by carrying out a second extraction on the same sample. In all cases, at least 99% of the tin was removed in the first extraction.

The effectiveness of the tin extraction procedure was confirmed by applying it to a tin amalgam of known concentration. The analysis agreed with the known concentration to within 1%.

The results for duplicate samples of the tin amalgam used in the evaporation rate study were 53 ppm and 51.5 ppm.

Sodium Amalgam

The sodium amalgam analysis was carried out in a manner similar to that for the tin amalgam with a slight difference in the first dilution. A first quick rinse of the amalgam was made using about 5 ml of distilled water, and then the amalgam was shaken with 2 ml of 3.7 N HCl for 5 minutes. The acid extract and the distilled water washings were combined and diluted to the 0-3 ppm concentration range. The results for duplicate samples of the sodium amalgam used in the evaporation rate study were 228 ppm and 229 ppm.

Lithium Amalgam

The lithium amalgam analysis was performed in a similar manner to the sodium amalgam analysis. The first dilution to the 0-10 ppm concentration range included a first quick extraction with 5 ml of distilled water, an acid extraction from shaking the amalgam for five minutes with 2 ml of concentrated HCl, and a final extraction with distilled water. Triplicate samples of the lithium amalgam used in the evaporation rate study gave 165 ppm, 165 ppm, and 161 ppm.

APPENDIX VI

THE EFFECTIVE PRESSURE ABOVE THE MENISCUS IN THE EVAPORATION EXPERIMENTS

To gain an insight into the pressure distribution and flow of mercury vapor in the evaporation chamber, calculations based on the situation depicted in the accompanying diagram were carried out. This represents a mercury meniscus of area A cm^2 and at a temperature T °C from which evaporation is taking place into an otherwise evacuated tube, diameter d. The lower end of the tube is cooled so that condensation of the vapor occurs on the tube walls at a distance x below the meniscus. The temperature at the point of condensation is T_c.

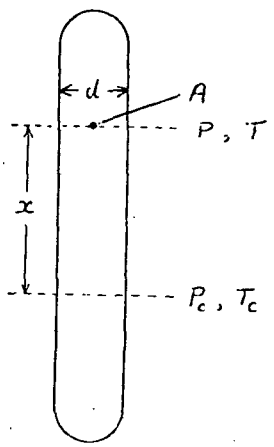

The values used in the calculations were, as far as possible, based on measured quantities. Thus the internal diameter of the tube was known to be about 4.6 cm, the distance x as assessed in actual experiments was about 12 cm, and, since the mercury condensed as crystals, the temperature at the point where condensation occurred was less than -38.9°C. The pressure at all points above the level of the meniscus was considered to be at the constant value P, while the pressure P_c and the pressures at all points below the condensation level were negligible ($< 4 \times 10^{-4}$ N/m^2).

Rate of Evaporation

Under these conditions outlined, the total rate of evaporation R from the meniscus could be calculated from equation (3). For pressures given in torr:

$$R_e = G \cdot A = 5 \cdot 833 \cdot 10^{-2} \cdot (Psat - P) \cdot \left(\frac{M}{T}\right)^{\frac{1}{2}} \cdot A \quad g \cdot sec^{-1}$$

For mercury (M = 200), this expression can be reduced to:

$$R_e = \frac{0.825\ (Psat - P)\ A}{(T)^{\frac{1}{2}}} \quad g \cdot sec^{-1}$$

Rate of Flow of Vapor

The rate of flow Q of the mercury vapor from the meniscus level to the condensation level is given by:

$$Q = F\ (P - P_c)$$

where F is the conductance of the tube (4). For a short tube, F may be calculated from:

$$F = 3638K\ (\text{Area}) \cdot \left(\frac{T}{M}\right)^{\frac{1}{2}}\ \ cm^3 \cdot sec^{-1}$$

where K is a constant dependent on the length-to-radius ratio of the tube. For a tube of radius 2.3 cm, effective length for flow, 12 cm, Clausing's calculations (4) show K to be 0.31. Therefore, for mercury (M = 200):

$$F = 1330\ (T)^{\frac{1}{2}}\ \ cm^3 \cdot sec^{-1}$$

and:

$$Q = 1330\ (T)^{\frac{1}{2}} \cdot (P - P_c)\ \ torr \cdot cm^3 \cdot sec^{-1}$$

$$= \frac{4.28\ (P - P_c)}{(T)^{\frac{1}{2}}}\ \ g \cdot sec^{-1}$$

Calculation of P

In the steady state, the rate of flow of vapor down the tube will be equal to the rate of evaporation. By equating Q with R_e, it may be shown that:

$$(P - P_c) = 0.193\ (Psat - P) \cdot A$$

so that P may be calculated if Psat, P_c, and A are known. Since P_c is negligible as compared to P, then P may be written as:

$$P = \frac{0.193 \cdot A \cdot Psat}{1 + 0.193 \cdot A}$$

Further, if A = 0.25 cm^2:

$$P = 0.046 \cdot Psat$$

or, if A = 0.50 cm^2:

$$P = 0.088 \cdot Psat$$

Thus, it can be seen that, if A is constant, P is a constant fraction of Psat. Also, to a good approximation, the ratio P/Psat is proportional to the meniscus area A. For most of the measurements made in connection with

the present work, A was about 0.25 cm^2. Thus, these considerations suggest that P should have been about 1/20 of Psat for most experiments. This was the case as can be illustrated with data from the first measurements on pure mercury (Table 1). For the third point of Run 4, the area was 0.25 cm^2, T was 48.0°C and Psat for this temperature is known to be 1.60 N/m^2 (12.0×10^{-3} torr). The pressure P as deduced from the ionization gauge reading using the calibration factor of 102 was 8.3×10^{-2} N/m^2 (6.2×10^{-4} torr). Thus, the value of P/Psat was 1/19.4 and close to the approximate value of 1/20. This degree of agreement confirms that the measured pressures were in the expected range, though the calculations by which the ratio P/Psat was deduced cannot confidently be expected to be correct to within better than about ± 25%. This is because of the difficulty of calculating the flow conductance precisely when evaporation is taking place from a point source in a tube which is partially blocked by a smaller tube projecting through its wall.

DISTRIBUTION LIST - CR 120884

General Electric Company
Missile and Space Division
Valley Forge Space Technology Center
P. O. Box 8555
Philadelphia, Pennsylvania 19101
Attn: S. Weinberger — 1 copy

Hughes Aircraft Company
Space Systems Division
Los Angeles, California 90009
Attn: R. B. Clark — 1 copy

National Aeronautics and Space Administration
Lewis Research Center
21000 Brookpark Road
Cleveland, Ohio 44135
Attn: R. R. Lovell (M.S. 54-3) — 2 copies
J. R. Danicic (M.S. 500-313) — 1 copy
S. G. Jones (M.S. 54-3) — 1 copy
E. P. Symons (M.S. 500-318) — 30 copies

Poly Scientific Division
Litton Industries
1111 N. Main Street
Blacksburg, Virginia 24060
Attn: W. O'Brian — 1 copy

NASA Scientific and Technical Information Facility
Box 33
College Park, Maryland 20740
Attn: NASA Representative — 2 copies

National Technical Information Service
Springfield, Virginia 22151 — 40 copies